Dissertation

submitted to the
Combined Faculties for the Natural Sciences and for Mathematics
of the Ruperto-Carola University of Heidelberg, Germany
for the degree of
Doctor of Natural Sciences

Presented by
M.Sc. Cancer
Jin Wang
born in Lanzhou, China
Oral examination: 13th February 2019

Transcription factor Zas1:
investigating its role in fission yeast

Referees:

Dr. Péter Lénárt

Prof. Dr. Elmar Schiebel

Summary

The reshaping of interphase chromatin into rod-shaped mitotic and meiotic chromosomes is an essential part of the eukaryotic cell cycle. This process is promoted by condensin and topoisomerase II. However, various studies indicated that these two components are not sufficient to achieve proper chromosome condensation. A previous screen for novel condensation factors in fission yeast identified Zas1, a C_2H_2 zinc-finger transcription factor, as a key regulator of chromosome condensation. Although Zas1 has been shown to regulate the expression of a number of essential genes, the major genetic pathways controlled by this transcription factor have remained unknown.

In this thesis, I describe the results of a synthetic genetic array (SGA) screen to reveal the genetic interaction network of *zas1* by defining phenotypic relationships between genes. I present genetic interactions of *zas1* with *clr4*, *mde4*, *csm1* and *mug185*, which encode histone-lysine-N-methyltransferase, microtubule-site clamp monopolin complex subunits and DnaJ protein respectively. Using a multicopy suppressor screen, I discovered that overexpression of the spliceosomal subunit gene *usp101* rescues the temperature-sensitive phenotype of a *zas1* mutant. I present evidence that Zas1 binds the promoter of *usp101* and show that both mRNA and protein levels of *usp101* are decreased in a *zas1* mutant. Furthermore, transcriptome profiling reveals a drastic splicing defect in the *zas1* mutant, which can be recovered by *usp101* overexpression. In summary, my thesis reveals that Zas1 is a key regulator of *usp101* transcription and thereby controls the cellular splicing machinery.

Zusammenfassung

Die Organisation von Interphase Chromatin in mitotische und meiotische Chromosomen ist ein essentieller Bestandteil des eukaryotischen Zellzyklus. In diesem Prozess überehmen Condensin und TopoII die Hauptrollen. Mehrere Studien haben jedoch gezeigt, dass die beiden Faktoren alleine nicht hinreichend sind, um Chromosomen Kondensation zu erzielen. Im Vorfeld dieser Arbeit wurde mittels eines Chromosomen Kondensations Tests in *S. pombe* der C2H2 Zinkfinger Transriptionsfaktor Zas1 mit Chromosomen Kondensation in Verbindung gebracht. Eine trunkierte Variante von Zas1 führt bei restriktiver Temperatur zum Absterben der Zellen. Zas1 kontrolliert die Expression zahlreicher essentieller Gene und evolutionär konservierte Domänen wurden bereits charakterisiert. Dennoch ist es unklar, wie genau die Mutation von Zas1 zu einem Absterben der Zellen führt.

In dieser Arbeit wurde mithilfe eines Tests basierend auf synthetischer Letalität nach genetischen Interaktionspartnern von Zas1 gesucht, um die Funktion von Zas1 zu erforschen. *clr4*, *mde4*, *csm1* und *mug185*, welche eine Histon-Lysin-N-Methyltransferase, Unterheinheiten der Mikrotubuli-Klammer Monopolin und das Dnaj Protein codieren, wurden als Interaktionspartner von *zas1* als Teil des Chromosomen Kondensations Netzwerks identifziert. Mithilfe eines Multicopy Suppressor Tests konnte gezeigt werden, dass die Überexpression von *usp101* die Temperatur sensitive *zas1-Ts34* Mutante retten kann. Im Vorfeld dieser Arbeit wurde außerdem gezeigt, dass Zas1 den Promotor von *usp101* bindet. In der Temperatur sensitiven *zas1-Ts34* Mutante sind sowohl Transkript als auch Proteinlevels von *usp101* reduziert. Dieses Ergebnis lässt darauf schließen, dass Zas1 die Transkription von *usp101* reguliert. Die Transkriptom Analyse der *zas1-Ts34* Mutante legte zudem einen drastischen Splicing Defekt offen, der durch Überexpression von *usp101* kompensiert werden konnte. Zusammenfassend konnte ich in dieser Arbeit zeigen, dass *usp101* eines der Hauptziele von Zas1 ist. Abwesenheit dieser Regulation in der *zas1-Ts34* Mutante führt deshalb zu weitgehenden Splicing Defekten, welche die Letalität der Mutante erklären.

Contents

Chapter 1 Introduction

1.1 The cells as the unit of life

The complexity of life is reflected by the extreme diversity of organisms, which come in different sizes and shapes, live in different environments and adapt distinct strategies to gain energy. However, all organisms originated from a common ancestor and diverged into the three main kingdoms classified today – bacteria, archaea and eukaryotes (Pollard et al., 2017). With the accumulation of information about the molecular mechanisms that underlie the function of the cell, remarkable similarities can be found at the biochemical level from species of different parts of the phylogenetic tree, although they have a stunningly different appearance and have been separated evolutionarily for a vast amount of time.

The smallest unit of the living organism is the cell, the place where diverse biochemical reactions for life function. For eukaryotes, cells have nucleus floated in the cytoplasm that is enclosed by a double membrane. In the nucleus, the genetic information is stored in nucleic acids molecular DNA, which is compacted into chromosomes by its association with histone and other proteins. Information is transferred from DNA to RNA and translated into large biomolecules with specific three-dimensional structure called proteins, which are responsible for wide range of cellular functions.

1.2 The cell cycle

Cells reproduce by duplication and division. The series of events that take place sequentially in this process is called the cell cycle. Researches on mammalian cells and model organisms such as yeast have revealed that all eukaryotes share similar mechanisms to control the cell cycle (Nurse 2000; Fantes 1977). The cell cycle can be divided into four phases – G1, S, G2 and M phases (Morgan 2007).

M phase consists of mitosis and cytokinesis. The term mitosis (mito for 'thread' in Greek) was coined by Walther Flemming in 1878, when he first observed stained chromosomes that segregated to opposite poles of the cell. Cytokinesis defines the process that constricts the cell equator and separates chromosomes and cytoplasm from the mother cell into two daughter cells.

Mitosis can be subdivided further into five phases: prophase, prometaphase, metaphase, anaphase and telophase. The condensation of chromosomes marks the beginning of the prophase and the two poles of the mitotic spindle are formed. In many species, prometaphase begins with the breakdown of the nuclear envelope and random attachment of chromosomes to microtubules. Metaphase is defined once chromatid pairs have aligned at the equator of the cell via the connection between microtubules and kinetochores. During anaphase, the two chromatids separate towards the two opposite poles of the spindle and the nuclear envelope is reformed during the telophase.

Following cytokinesis, cell can enter a new cell cycle or exit the cell cycle. Most differentiated mammalian cells exit the cell cycle and enter a quiescent state (referred to the G0 phase) to carry out specific cellular functions. Cells in this phase are hence 'active' rather than 'dormant'.

G1, S and G2 phases are referred to as 'interphase' since this period of the cell cycle consists of cell growth and DNA replication as preparation for mitosis. As the first gap between the previous mitosis and a new round of DNA replication, cells in G1 phase increase their mass by the uptake of nutrients. Stimuli are evaluated carefully by the biochemical control system as a restriction point. Cells replicate their DNA during S phase (Synthesis phase). The G2 phase is another gap between the DNA replication and mitosis. It has the final checkpoint before entry into mitosis.

1.3 Transcription and RNA processing

DNA serves as the static platform for the storage of genetic information. The first step in the use of the genetic information is the transcription from DNA into complementary RNA molecules by enzymes called RNA polymerases. RNAs are single-stranded chains of ribonucleic acids and can adopt a variety of shapes and execute different functions (Alberts, 2014). Some RNAs are not translated into proteins but play regulatory or structural roles, including ribosomal RNA (rRNAs), transfer RNAs (tRNAs), small nuclear RNAs (snRNAs), small nucleolar RNAs (snoRNAs) and microRNAs (miRNAs). rRNA is the RNA constituent of ribosomes, which are the key machines to synthesize proteins. About 80% of the total RNA in eukaryotic cells is rRNA (Lodish H et al., 2000). tRNAs are another essential part of the translation machinery, serving as the link between mRNA and amino acids during protein synthesis. snoRNAs assemble into protein–RNA complexes and modify nascent rRNA transcripts to generate mature rRNAs. miRNAs are a class of small RNAs that function in gene expression regulation. snRNAs associate with small nuclear ribonucleoproteins to form the spliceosome, which is the core machinery for pre-mRNA splicing.

In prokaryotes, the primary transcripts transcribed from the protein-coding DNA are immediately used for protein translation. In contrast, in eukaryotes, the stretch of DNA that encodes a protein will first be transcribed into precursor messenger RNAs (pre-mRNAs). Mature messenger RNAs (mRNAs) that qualify for protein translation are only available after several processing steps including 5' end capping, 3' end poly adenosine addition and splicing (Hocine S & Singer R., 2010)

The 5' end of pre-mRNAs is modified by a 7-methylguanosine moiety (5' cap) to protect mRNA from degradation and facilitate the alignment of mRNAs in ribosomes during protein synthesis. At the 3' end, by recognizing two highly conserved motifs in the pre-mRNA- AAUAAA and GU-rich sequences, the 3' end processing complex, which consists of more than 20 proteins, assembles and cleaves the pre-mRNA from the transcription complex. The released transcripts are subsequently added with a chain of adenosine (A) residues (150-250 A in mammalian cells and 55-90 A in budding yeast) at the 3' end that is defined as 3' polyA tail, signalling for the end of the transcription (Brown C. E. & Sachs A., 1998).

1.4 The splicing machinery and usp101

The third main pre-mRNA processing event is RNA splicing. In metazoans, including humans, the vast majority of genes across the genome contain both expressed sequences (exons) and intervening sequences (introns). Introns are intragenic regions in DNA and RNA sequences that are removed during mRNA maturation and will thus not be translated into protein. The remaining expressed sequences are joint together for protein translation and are hence defined as exons. By joining different exons, alternative splicing provides a strategy to generate a multitude of proteins from a limited number of genes. The key machine to execute the splicing is a dynamic complex composed of small nuclear RNAs (snRNAs) and proteins, named the spliceosome.

The function unit in the spliceosome is small nuclear ribonucleoprotien (snRNP) consisting of snRNA combined with protein. The spliceosome has five Uridine-rich (U-rich) snRNPs (U1, U2, U4/U6 and U5) and approximately 100 other auxiliary proteins (Wahl et al. 2009; Matera & Wang 2014). Each snRNP contains specific uridine-rich small nuclear RNAs (snRNAs), unique associated proteins and a common component called Smith (Sm) proteins that assemble into a hetero-heptameric ring and serve as the core of the snRNP particle. In the complexes (snRNPs), the snRNAs rather than the proteins function catalytically. In premRNA, the conserved sequences located at the 5’ and 3’ ends of intron as the splice sites and the internal region around the branch point adenosine residue are signals for accurate recognition by U snRNPs to achieve catalysis.

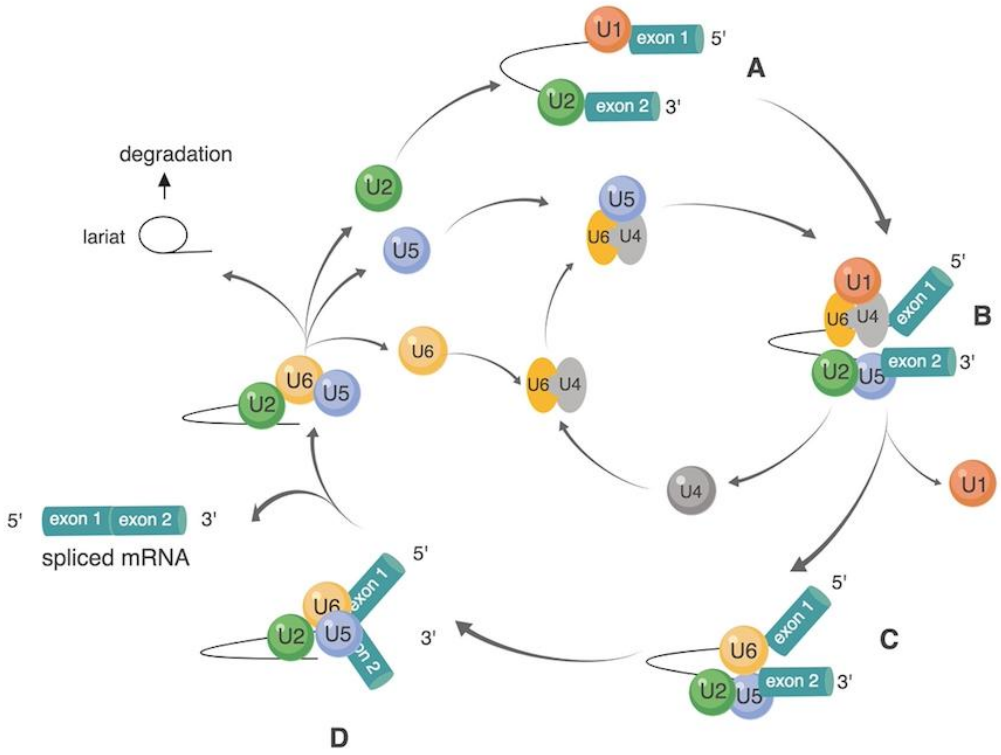

Figure 1.1 Assembly cycle of major spliceosome and step-wise splicing.

With recognization of splice sites, the U1 and U2 snRNP assembled onto the pre-mRNA adjacent to the 5' and 3' splice site resepctively and form the pre-spliceosome complex (A). Subsequent tri-snRNP complex composed of U4/U6 and U5 are recruited to the A to form the complex B. Along with a series of rearrangement, U1 and U4 snRNP are released to form the active complex C. The first catalytic splicing reaction is taken place and generates the complex D with a lariat-exon2 intermediate and free exon1. The second catalytic step is then carried out along additional rearrangements, generating the spliced exons and the lariat intron that is removed out from the pre-mRNA. The released U2, U5 and U6 snRNP are then recycled to join further rounds of splicing (graph adapted from (Collins et al. 2009)).

Although the chemical reactions involved in the splicing are simply two trans-esterification steps, the biochemical basis is much more complicated. The splicing event begins with base pairing between the U1 snRNA and the 5' splice site with support of the associated proteins. Subsequently, the U2 snRNA pairs with sequences surrounding the branch point that is 15-20 nucleic acids upstream to the 3' splice site (Collins et al. 2009; Matera & Wang 2014; Wahl et al. 2009). Upon assembly of the U4/U6 complex and U5 snRNPs, the adenosine in the middle of the branch point region is brought into close proximity of the 5' splice site. The site is then attacked by the 2' hydroxyl group on the adenosine. Subsequently, the exon 1 is free and the intron is left as a circularized intron called lariat. In the second catalytic step, the free exon 1 attacks the 3' splice site. By which the exons are ligated. The intron lariat is then released and degraded afterwards (Figure 1.1).

As the current model of spliceosome action shows, splicing initiates from the recognition of the 5' end of the intron by base-pairing between the U1 snRNA moiety of the U1 snRNP and the pre-mRNA substrate (Wahl et al. 2009; Matera & Wang 2014; Hofmann et al. 2010; Patel & Bellini 2008). In addition to the U1-snRNA and the Sm proteins, the U1 snRNP consists of U1-specific proteins: U1-A, U1-C and U1-70K (Patel & Bellini 2008). In human cells, U1-70K is a polypeptide chain that is composed of an N-terminal, an RNA binding and a C-terminal domain. It is an essential part for the functional U1-snRNP, since it is able to bind the U1-RNA via the stem loop 1 and its N-terminal domain is necessary and sufficient for the binding of U1-C and the core Sm proteins (Faustino et al. 2003; Kornblihtt et al. 2013; Matera & Wang 2014). In *Schizosaccharomyces pombe*, 43% of protein coding genes contain intron which is significantly different from the genome feature from budding yeast (5% of its protein coding gene) (Newo et al. 2007). Gene *usp101* encodes the homolog of U1-70K (Newo et al. 2007) in *S. pombe*. Therefore, Usp101 is essential for reliable splicing and hence cell viability in fission yeast.

1.5 Chromatin organization and remodeling

The diameter of the nucleus in eukaryotic cells is only roughly one of half million of the length of DNA molecules (Edens et al. 2013; Lammerding 2011; Ou et al. 2017) and thus the chromosome must be highly compacted in the cell. Several layers of folding are required to achieve sufficient compaction. The first layer is accomplished by wrapping 146 bp of DNA around the histone octamer, which is composed of two copies of H2A, H2B, H3 and H4 core histone proteins (Richmond 1984; Cutter & Hayes 2016). The 1.67 left-handed superhelical turns of DNA on histones form the nucleosome core particle, which has a diameter of 11 nm. The chromatin with nucleosomes appears as beads-on-a-string in electron micrographs and provides not only a seven fold compaction compared to the naked DNA, but also serves as a platform for epigenetic covalent modification for gene regulation. The chromatin is then further shortened for another six to seven fold via mechanisms that are controversial as to date. It has been proposed that highly dynamic and irregular looping and coiling are involved in the packaging rather than previous prediction that fibers with diameter of 30 nm are formed.

Arrays of nucleosomes not only compact the DNA, but also set barriers for the transcription machinery and other proteins that need to access the genome. Thus, gene activation requires dislocating or unwrapping nucleosomes (Lorch et al. 1987). Numerous interactions between DNA and the octamer histone core provide nonspecific but tight contacts that is feasible to be remodeled for a dynamic binding.

Chromatin remodeling processes can loosen the nucleosomes and make easier access to the transcription machines by modification of chromatin structure. Two main strategies to achieve chromatin remodeling are based on 1) histone modification and 2) the activity of chromatin remodeling complexes. Covalent modification on histone protein includes methylation, acetylation, ubiquitylation, phosphorylation and sumoylation (Bannister & Kouzarides 2011). Corresponding modifying enzymes are recruited by regulatory proteins and often target the lysine residues (K) of the histone tails. Chains of nucleosomes with methylations on lysine 9 and lysine 27 of histone H3 (H3K9me3 and H3K27me3) are signals for silent chromatin. Acetylation on lysine 4 residue of histone H3 or lysine 8 of histone H4 (H3K4ac and H4K8ac) and H3K4me are markers for active chromatin. Chromatin remodeling complexes can utilize the energy from ATP hydrolysis to destabilize the association between DNA and histones to move or restructure nucleosomes (Vignali et al. 2000).

1.6 Chromosome compaction

In addition to the packing of DNA into chromatin during interphase, further compaction during mitosis is essential to condense chromatin from an amorphous mass into rod-shaped chromosome to allow proper chromosome segregation (Flemming 1878).

The mechanism of the chromatin compaction is highly debated. There are two popular historical models that attempt to describe the process of chromosome condensation. The first model suggests that chromatin fold in a hierarchical manner (Maeshima & Eltsov 2008; Hansen 2002), forming a consecutive higher-order structure of a 300-nm fiber from a 30-nm fiber that originates from the 11-nm nucleosome chain. The second model suggests the existence of a 'chromosome scaffold'. The chromatid fiber is compacted by forming loops extruding from anchors at the scaffold. Recent chromosome conformation capture experiments and polymer-based simulations have supported the model of a dynamic scaffold (Kschonsak & Haering 2015; Fudenberg et al. 2017; Fudenberg et al. 2016). It is also conceivable that these two models exist in parallel and describe different phases of the chromosome condensation process.

Two chromosomal components - topoisomerase II (topo II) and condensin - have been found to play key roles during chromosome condensation. Condensin is a pentameric protein complex that consists of two SMC (structural maintenance of chromosome) proteins (Smc2 and Smc4), one kleisin subunit and two subunits of protein composed of HEAT repeats. SMC proteins contain a hinge domain and an ATPase head domain, which are separated by an anti-parallel coiled coil. Two SMCs associate with each other via the hinge domain and form a ring-like structure by the interaction of the two ATPase head domains with the kleisin subunit (Onn et al. 2007; Neuwald & Hirano 2000; Anderson et al. 2002). There is evidence that the condensin ring might encircle chromatin fibers topologically (Cuylen et al. 2013; Cuylen et al. 2011). Ycg1, one of the HEAT-repeat subunits in budding yeast, has been found to form a DNA-binding site together with the kleisin subunit (Kschonsak et al. 2017).

Topoisomerase II is an enzyme that controls DNA supercoiling and catenation by transiently cutting the DNA double strand. Like condensin, it has been reported to localize to the chromosome scaffold (Maeshima & Laemmli 2003; Earnshaw & Heck 1985; Gasser et al. 1986) and play a role for proper chromosome condensation (Uemura 1987, Kireeva et al. 2004).

Although chromosome condensation is severely affected when condensin is inactivated in both budding yeast and fission yeast, knock-down of condensin in DT40 chicken cells or in *Caenorhabditis elegans* does not prevent chromosome compaction to appreciable levels, although it leads to a loss of chromosome integrity (Hudson et al. 2003; Vagnarelli et al. 2006; Kirsten A. Hagstrom 2002). Inhibition of topoisomerase II in mammalian cells leads to compromised chromatin condensation (Gorbsky G. 1994), whereas low expression of topoisomerase II in *Drosophila* impairs chromosome segregation without an evident condensation defect (Chang 2003).

1.7 The *zas1* gene

The discrepancies between these observations prompted the hypothesis that there must exist yet-to-be-identified players that induce mitotic chromosome condensation. To identify novel condensation factors, a previous PhD student, Boryana Petrova, had established a live-cell assay that monitors chromosome condensation quantitatively in the fission yeast *Schizosaccharomyces pombe* (Petrova et al. 2013). In this assay, two genomic loci on the same arm of a fission yeast chromosome had been labeled fluorescently. By measuring the three-dimensional distance of the fluorescent loci continuously as cells pass through mitosis, chromosome condensation could be tracked. With this assay, a random UV mutagenesis screen was conducted to search for mutants that have defects in chromosome condensation.

Three independent temperature-sensitive alleles of *zas1* were found with chromosome condensation defects in the screen. The *zas1* gene had first been described by Okazaki et al (Okazaki & Niwa 2000a) as an essential gene that encoded a protein with two C_2H_2 zinc-finger motifs. A subsequent biochemical characterization from another PhD student, Christoph Schiklenk, has shown that Zas1 is a transcription factor with a transactivation domain motif that is essential for function. A nuclear localization sequence (NLS) and two C_2H_2 zinc finger motifs locate near the N terminal. In C_2H_2 zinc finger motif, paired cysteine (C) and histidine (H) residues coordinate with a zinc atom to form a featured secondary structure that serving as a platform for interaction between DNA and the finger. The C terminal, where all mutations generated from the UV-mutagenesis locate, has sequence homology of fungal transcription factors.

Analysis of genome-wide binding sites by chromatin immunoprecipitation combined with next-generation sequencing has revealed that, functioning as a transcription factor, Zas1 binds DNA in a sequence specific manner and regulates expression of a series of genes (Table 1.1), including *cnd1*, which encodes the Cnd1 HEAT-repeat subunit of the fission yeast condensin complex.

Surprisingly, however, restoring normal expression of *cnd1* was not sufficient to rescue the growth defect of a *zas1* temperature-sensitive mutant at the restrictive temperature. This suggested that Zas1 must have an essential function for cell proliferation that goes beyond activating the expression of *cnd1*.

Table 1.1 Top ranked genes with sequence specific Zas1-binding peak at promoter region (Schiklenk et al. 2018, Pombase)

Gene Name	Annotation	Essential
SPBC1652.02	Predicted as transmembrane amino acid transporter	No
peg1	CLASP family protein related to microtubule regulation	Yes
SPAC644.09	prediced as protein binds pyridoxal phosphate	No
tom22	Tom22-subunit of mitochondrial TOM complex	Yes
pmo25	mo25 family protein regulating cell polarity	Yes
pyp3	phosphatase Pyp3	No
cnd1	condensin complex subunit Cnd1	Yes
SPAC1B9.03c	predicted as RNA-binding protein functioning in ribosome assembly	Yes
teb1	transcription factor Teb1	Yes
pob1	Boi family protein implicated in cell tip growth	Yes
pre5	Pre5-subunit of 20S proteasome complex	Yes

1.8 Fission yeast as model organism

Schizosaccharomyces pombe is a unicellular eukaryote with a rod-like shape. Haploid cells have a size of 7–14 μm in length and 3-4 μm in width. *S. pombe* cells grow through linear extension of the cell tip and produce daughter cells by medial fission (hence its classification as fission yeast) (Hagan et al., 2016, Matthieu Piel 2009). In the presence of sufficient nutrients, *S. pombe* cells can undergo a continuous cell cycle with a generation time of 2.5 h at 30°C. It is classified as ascomycete yeast, since it forms an ascus around sexual spores. The analysis of proteomic and DNA sequence data suggests that *S. pombe* is more ancient than *S. cerevisiae*. About 420 million years of evolution separates these two yeasts, which is in the same order as the evolutionary distance between *S. pombe* and humans (Sipiczki 2000; Heckman et al. 2001).

Researches with *S. pombe* as a model organism date back to the 1940s (Hoffman et al. 2015) and focus mainly on the sexual cycle (Bresch et al. 1968; Egel 1973) and cell division (Lee & Nurse 1987; David Beach 1982; Nurse & Bissett 1981; Paul Nurse 1975). The homothallic strain 968 h^{90} and two heterothallic strains, 972h^{-} and 975 h^{+}, are derived from a single isolate (Leupold 1949, Strzyz 2018). They are distributed to laboratories all over the world since then and served for almost all genetic researches on *S. pombe*.

Currently for *S. pombe* there are 5054 reported protein coding genes. This number is lower than that 5,821 protein coding genes annotated in *S. cerevisiae*. Yet, 338 protein coding-genes that are conserved between *S. pombe* and vertebrates but absent in *S. cerevisiae*, whereas only 179 genes are conserved between *S. cerevisiae* and vertebrates and absent in *S. pombe* (Pombase, SGD, Valerie Wood 2016; Aravind et al. 2000). This indicates relative closer relationship between *S. pombe* and vertebrates. Besides, large centromeres in *S. pombe* with central core sequence surrounded by a number of outer repeats are also more reminiscent of the centromeres in human (Kniola B. 2001). Therefore *S. pombe* is also called small mammalian cell from the model organism perspective.

The genome size of *S. pombe* is 13.8 Mb and is organized into three chromosomes of the sizes of 5.7, 4.6 and 3.5 Mb (Wood et al. 2002; Lock et al. 2018). In comparison, *S. cerevisiae* has genome of 12.5 Mb that are distributed in 16 chromosomes (SGD). The longest budding yeast chromosome (chromosome I, 1.5 Mb) is less than half the size of

the shortest fission yeast chromosome (chromosome III, 3.5 Mb). This feature makes *S. pombe* the better suited yeast species to investigate chromosome condensation in my study.

1.9 SGA design and procedure

Genetic interaction is a widely used technique to characterize the relationship between two genes. When the phenotype of double mutants cannot be explained only based on the combined effects of the individual mutants, a genetic interaction between these two genes can be defined (John C. Lucchesi 1968; Avery & Wasserman 2013; Hartman et al. 2001).

Genome-wide genetic interaction analysis was pioneered in *Saccharomyces cerevisiae* upon the completion of a haploid deletion strain library covering ~5,000 non-essential genes (Giaever et al. 2002) and development of an SGA platform (Tong et al. 2001) to facilitate the automation of the genetic interaction studies. The SGA platform was later further developed for *S. pombe* using the commercially available haploid deletion library (Kim et al. 2010). This library (Bioneer haploid deletion library V5) covers 3,420 deletions of non-essential genes using the *kanMX4* antibiotic selection marker. The deletion library covers 95.3% of the non-essential genome of *S. pombe*.

A robotic system (ROTOR HDA, Singer Instrument) has been developed to facilitate the automated replica-plating steps in a high-throughput scale. The query strain to be crossed to the deletion library usually carries a mutation or deletion of the gene of interest at the endogenous locus and is tagged with the *natMX6* selection marker. The query strain of the h^- mating type is then arrayed and crossed with the h^+ deletion strains in the library to form heterozygous diploids. After sporulation and germination, series of selection steps based on the selection marker are performed to isolate the haploid double mutants (Figure 1.2).

The experimental platform PEM-2 (Pombe Epistasis Mapping) has been developed by Assen Roguev et al (2007) to facilitate the generation of double mutants compatible for SGA in *S. pombe* (Figure 1.3). Specific selection markers and mutations have been engineered into the query strain to ease the selection procedure and make it adaptable for query strains with temperature-sensitive (ts) alleles.

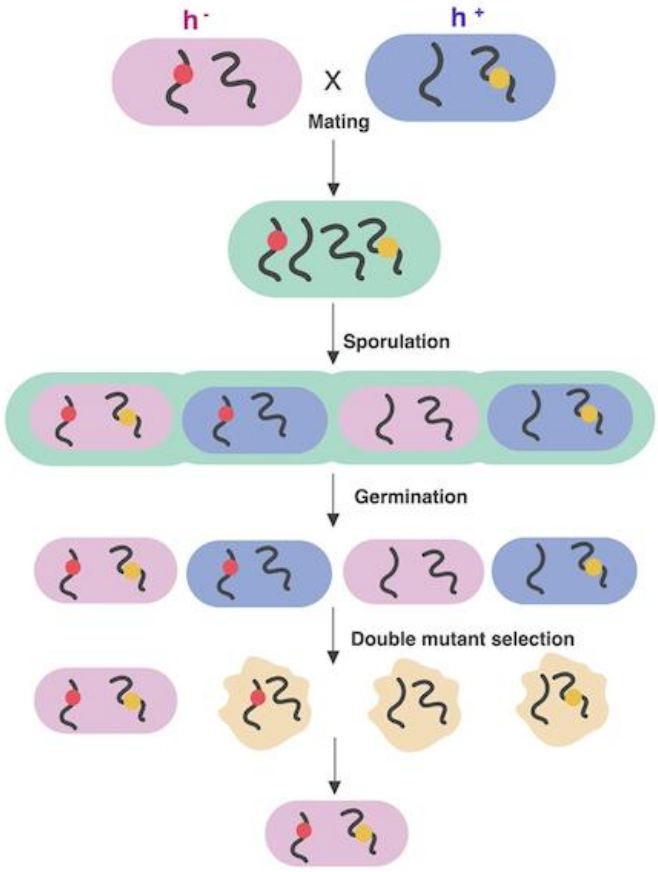

Figure 1.2 Synthetic genetic array (SGA) methodology.
Query strain (h-) was crossed with deletion library (h-) and underwent subsequent meiosis and sporulation. Haploid double mutant was obtained after series of selections. The whole procedure can be carried out in high throughput manner using robotic platform.

Mating on nitrogen deprived medium, *S. pombe* heterozygous diploids form and immediately undergo meiosis and sporulation. Three types of cells exist after this step: haploid meiotic products, unmated parental cells and non-sporulated diploid cells. As the mating process is conducted in the high throughput manner in the SGA analysis, there frequently exists a small population of diploids that did not sporulate. These non-sporulated diploids would survive the antibiotic selection step and even show a higher resistance to stress than haploid cells. The non-sporulated diploids would hence over grow the haploid species. Furthermore, haploid cells with different mating type in the same population will re-mate and form new diploids during the selection. Thus key selections are implemented in the PEM2 system to eliminate all the contaminated species: 1) antidiploid selection (ADS); 2) mating-type selection (MTS) and 3) double mutant selection (DMS).

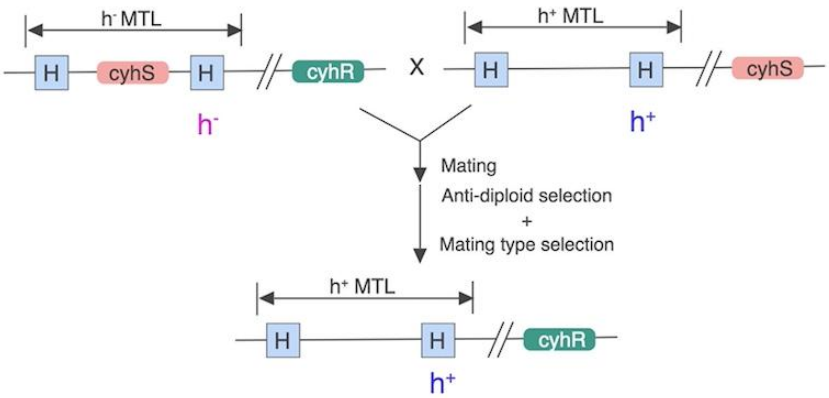

Figure 1.3 PEM-2 strategy for double mutant selection: in the PEM-2 strain with a cyhR allele expressed from the endogenous locus and a cyhS allele engineered in the h- mating type locus, the h- haploid processes the genotype mimicking a heterozygous diploid. After meiosis and double mutant selection with antibiotic and cycloheximide, the only survived cells would be the meiotic products with double mutations and single mating type (h^+) (graph adapted from (Roguev et al. 2007)).

In PEM-2 strategy, the antidiploid selection is achieved via manipulating gene *rpl42*. The S. pombe *rpl42* gene encodes the large ribosomal subunit L36/L42. The P56Q mutation on rpl42 confers recessive resistance to cycloheximide to the strain, which is otherwise naturally sensitive to cycloheximide (Roguev et al. 2007). In the PEM2 query strain, the endogenous *rpl42* obtained P56Q mutation. Besides, another wild type *rpl42* (*rpl42*$^+$) was integrated into the h- mating type locus of the query strain. Thus the genotype of h^- query strain mimics a heterozygous diploid as *rpl42*$^+$/*rpl42-P56Q*. This will confer the h^- strain with the sensitivity to cycloheximide and by which to achieve the mating type selection and prevent re-mating during the screening. As the h^+ haploid deletion library only contains endogenous *rpl42*$^+$, after mating with the h^- query strain, the unsporulated diploid cells will be sensitive to cycloheximide as they would contain *rpl42*$^+$/*rpl42-P56Q*. And any unmated parental cells, as both h^+ and h^- cells contains *rpl42*$^+$, would be eliminated by the cycloheximide treatment as well. So with addition of cycloheximide, both mating-type and anti-diploid selection can be achieved simultaneously. Only h^+ haploid that result from sporulation of the mated strains, but neither parental haploid, sporulated h^- haploid, nor diploid strains will be able to proliferate in the presence of cycloheximide. Double mutant cells can then be selected by adding antibiotics that correspond to the antibiotic resistance selection markers in the query and library strains.

1.10 Objectives of this thesis

Zas1 has been recently shown to function as a transcription factor that controls the expression of the condensin subunit gene *cnd1* and several other genes, but downregulation of neither of these genes could explain the temperature lethal phenotype of *zas1* mutants. The aim of my study was to further characterize Zas1 to understand its specific mechanism of action. Understanding Zas1 function would provide insights into how mitotic chromosomes are timely formed at the onset of mitosis.

To reveal the function of a gene with limited annotation, I started with systematic genetic approaches such as synthetic genetic screen and suppressor screen to collect information of the network of Zas1 function. With the information of *zas1* direct/indirect targets and interaction partners, the research focus is narrowed down to the filtered pathway and gene. Specific assays were designed accordingly and revealed the gene that is directly responsible for the phenotype in *zas1* mutant.

Chapter 2 Results

2.1 Identifying genetic interaction partners of zas1 by synthetic genetic array (SGA) screening

2.1.1 SGA strategy

To begin my studies, I performed SGA to identify genome-wide interaction partners of *zas1*. I selected the ts allele of *zas1* (*zas1-Ts34*) to construct the mutant query strain, since this mutation results in a robust temperature-sensitive phenotype according to a previous report (Schiklenk et al. 2018). Of all *zas1* mutants tested, this allele has the least impact on cell growth at the permissive temperature 25°C, while resulting in the most striking temperature lethal phenotype at the restrictive temperature 34°C. In the *zas1-Ts34* mutant, a nonsense mutation at amino acid position 712 results in the mutation of a tryptophan residue to a stop codon (W712X) (Okazaki & Niwa 2000b). For the SGA, I created the *zas1-Ts34* mutation by truncating the *zas1* gene at position 712 and added the *natMX6* selection marker (Figure 2.1).

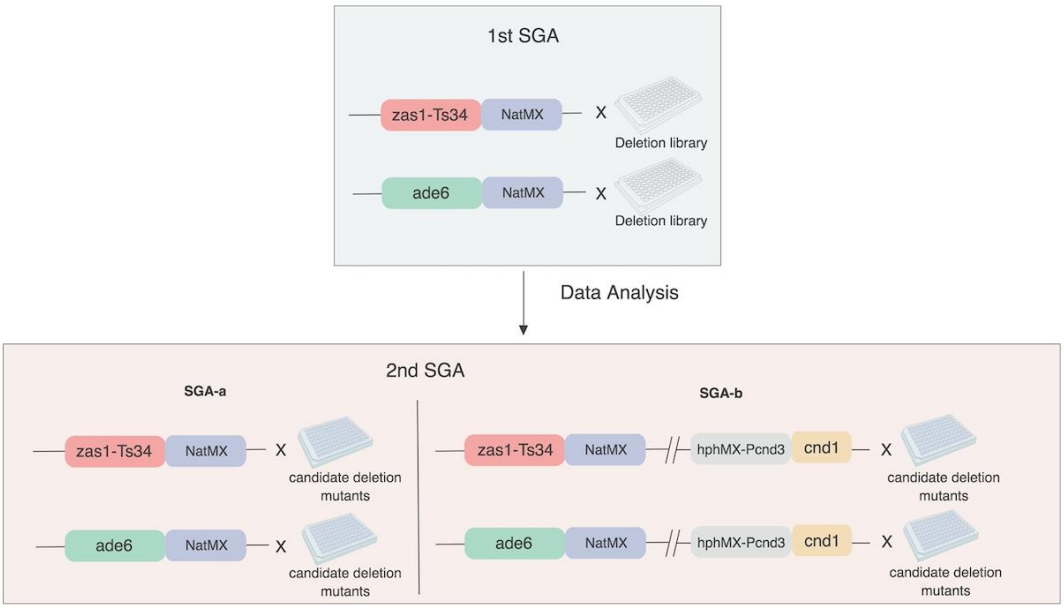

Figure 2.1 Pipeline of two rounds of SGA screen: SGA with control query was conducted in parallel with query SGA. In the first round of SGA, *zas1-Ts34* mutant was crossed with the haploid deletion library. With double mutant isolation, primary candidate hits that have negative genetic interaction with zas1 were obtained after data analysis. A second round of SGA was conducted for query strains *zas1-Ts34* (SGA-a) and *zas1-Ts34* P_{cnd3}-*cnd1* respectively (SGA-b), crossing with haploid deletions of candidate genes obtained from the first round of SGA.

I designed two rounds of SGA to isolate genetic interaction partners of *zas1*. The aim of the first round of SGA was to reveal general genetic interaction partners of *zas1* in a genome-wide manner, thus the query strain carried only the *zas1-Ts34* mutation. The second SGA was designed to isolate genetic interaction partners of zas1 that are exclusively related to *cnd1*, and thus might most likely be involved in the chromosome condensation process but not in other functions of *zas1* (Figure 2.1). The query strain for the second analysis therefore carried the *zas1-Ts34* and a replacement of the *cnd1* promoter that decouple the expression of *cnd1* from Zas1's regulation.

2.1.2 First round of SGA

For the first SGA (Figure 2.2A), arrays of the *zas1-Ts34* query strain were mated with all mutants in the haploid h^+ *S. pombe* deletion library on SPAS media for 3 days at 25°C, during which cells underwent meiosis and sporulation. After germination on YE5S rich media for 2 days, undesired cells were eliminated by replica-plating on media with cycloheximide. Geneticin was added in this step to improve the selection efficiency (Roguev et al. 2007). Colonies were then replica-plated onto plates with cycloheximide, geneticin and clonNAT to select for haploid double mutants at 25°C, 30°C, 34°C and 37°C respectively. The reason for selecting the 384 format rather than the 1546 format is that previous trial runs showed that cells in the 384 format had more nutrition to grow and each colony had more space to expand, resulting in a larger dynamic range of colony size and hence more confidence in the data analysis.

Deletion of the *ade6* gene with the *natMX6* marker in the same background strain was used in parallel as control for normalization and interaction value calculation purposes (Rallis et al. 2017).

For data collection, all plates were photographed after the double mutant selection step. Colony size, a proxy for mutant fitness, was used as the readout for the screen and analyzed with the web server SGATools (Wagih et al. 2013). This software platform first identifies colonies on the plate image based on the pixel intensities and then counts pixels from each colony as a measurement of the colony size. This data was then further analyzed using in-house SGA analysis tools developed by StJohn Townsend in Bähler lab (UCL, UK) (script unpublished, Rallis et al. 2017).

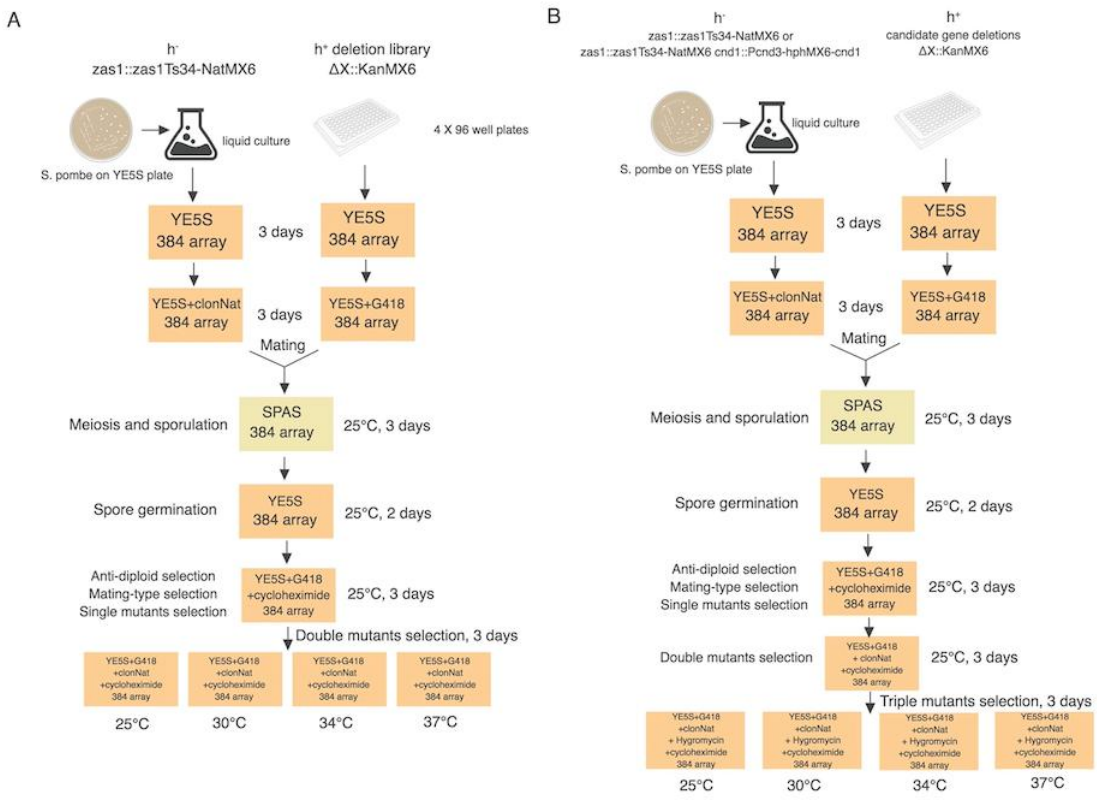

Figure 2.2 Representation of SGA pipeline. (A) All of manipulations for the arrayed plates were conducted with robotic platform ROTOR. In the first round of SGA aiming to screen genetic interaction partner of zas1 at genome scale, single colony of the freshly grown query strain (h^-, PEM2-*zas1-Ts34*-natMX6) was inoculated in YE5S liquid media overnight and arrayed onto YE5S agar plates. Deletion library stored at -80°C was thawed and replicated onto the YE5S agar plates. Both query strain and deletion library strains were replicated from YE5S to YE5S+G418 respectively to ensure the existence of the dominant selection markers. After three days incubation at 25 °C, the arrayed query strain was crossed to h^+ deletion mutants arrays on SPAS agar plates. With three days incubation at 25°C the meiosis products generated were replicated to rich media YE5S for sufficient germination. The meiotic progeny were transferred to the media containing cycloheximide and Geneticin. The former reagent was added in to eliminate contaminated cell population. Geneticin was added to select for single and double mutants together. Double mutants were isolated by YE5S media contains cycloheximide and two antibiotics - Geneticin and clonNat at temperature 25°C, 30°C, 34°C and 37°C respectively. (B) In the second round of SGA, two SGA with query strain PEM2-*zas1-Ts34* and PEM2-*zas1-Ts34*-hphMX6-*cnd1*::P_{cnd3}-*cnd1* were performed in parallel. Procedure is similar to A), except one more layer of selection was added in. After single mutant selection, double mutant selection with cycloheximide, Geneticin and clonNat. In the triple mutants isolation step, progenies were transferred onto the YE5S medium with cycloheximide and three antibiotics – Geneticin, clonNat and Hygromycin at four different temperatures.

2.1.3 SGA data analysis

Several experimental factors may introduce systematic variations to the colony size measurements during the arrayed genetic screens. These factors include the 'plate effect', which is the difference in the average colony size amongst different plates; the 'column and row effect' that accounts for the bigger colony size, which results from a better access to nutrients on some parts of the plates (e.g. at edges), and the 'spatial effect', which is caused by uneven growth medium surface on the plate. These variations were corrected by the SGA analysis software (Rallis et al. 2017).

Colony sizes were firstly normalized to the median size of each plate. Rescaling was then applied to each column and row to make their colony sizes comparable. This step was particularly important for colonies that were close to the edge of plates and thus had more nutrients available compared to cells at the center of the plate. Spatial smoothing was also performed to correct for variations in the plate surface.

In addition to the plate effects correction steps, several specific filters were implemented in the software to flag colonies that might be false positive. The first one was the 'linkage filter'. The colony size of double mutants of two genetically linked genes is usually small due to the rareness of the meiotic crossover between these two genes. Thus, the colony size might not accurately reflect the fitness of the desired double mutant. To compensate for this, genes that fell within 100 kb distance of the *zas1* gene were labeled as 'L' (linkage) and excluded from the data set to eliminate interaction values arose from genetically linked genes. Furthermore, colony sizes of the double mutants from the control *ade6Δ* SGA were evaluated independently and any colony size below 100 pixels was labeled 'S' (sick) and excluded from further analysis, since they were deemed to contain an amount of cell that was too low for accurate calculation. In addition, a Euclidean distance filter, defined by $\sqrt{control^2 + query^2}$, was applied to remove cases where both, the query and the control experiments, resulted in small double mutant colonies. According to previous experience (personal communication with the Bähler lab), many false positive hits arise from these cases because the relative variability of colony size for double mutants with small colonies is significantly greater than the ones with large colonies, presumably due to higher sensitivity of small colonies towards random effects such as differences in biomass during pinning. By definition of the Euclidean distance filter, only double mutants with small colonies in both query SGA

and control SGA will generate small value of the Euclidean distance. The cut-off for the Euclidean distance filter was set to 0.2 and any mutant that fell below this value was excluded from further analysis.

After normalization and filtering, genetic interaction values were determined based on the deviation of the observed double mutant fitness from the expected fitness. For this, a standard multiplicative score ($W_{ij} - W_i W_j$) (Wagih et al. 2013) was calculated for all the double mutants to indicate interaction values. W_{ij} represents the observed fitness of the double mutant; W_i is the median colony size of all strains in the *Δade6* SGA. This represents the fitness of single mutant library with the assumption that ade6 depletion does not affect the fitness of the library; and W_j represents the median fitness of double mutants in the query SGA, which serves as the estimation of the fitness of single query mutant, assuming that the genetic interaction events with the query gene across the genome are rare (i.e. most library single mutants are as fit as wild-type cells, thus most double mutants in the query SGA have the fitness of the query mutant).

Using this calculation, negative scores that represent negative genetic interactions were generated when the fitness of the double mutant was compromised stronger than that expected from the combined effects of the two individual mutants, or when cells didn't grow at all. This would, for example, be the case if two genes act in compensatory but independent pathways. Positive scores representing positive genetic interactions were generated when the double mutant displayed better growth than that expected from the sum effect of the two single mutants. Positive interactions can reflect a functional relationship within the same protein complex or same pathway (Baryshnikova et al. 2010; Forsburg 2001; Dixon et al. 2009; Ryan et al. 2012; Dixon et al. 2008).

Two biological replicates were performed for each round of SGA. Average of colony size from replicates was taken for interaction score calculation. For statistic representation, the logarithm at base 10 was applied to all the interactions scores, with +2 and −2 as the maximum and minimum values (Rallis et al. 2017). Besides, interaction scores with high variability among replicates were excluded. As reported (Wagih et al. 2013), a negative interaction that is strong enough to be recognized by naked eye usually has an interaction value below −0.3, which indicates that scores between −0.1 and 0.1 should be interpreted with caution, because they are unlikely to be reproducible. Rallis et al

(2017) recommends a cut-off at +0.15 and –0.15, which I used for the threshold for the genetic interactions in my study.

2.1.4 Validation of the SGA pipeline

Since single mutant strains of *zas1-Ts34* are not able to proliferate at 34°C and above, most of the double mutants obtained after the SGA selections step should also fail to proliferate at this temperature. If the counter-selection against parental strains were effective, colonies should only be able to grow on plates at 25°C and 30°C but not at 34°C and 37°C. This was indeed the case (Figure 2.3), which indicates that the series of selection steps were effective.

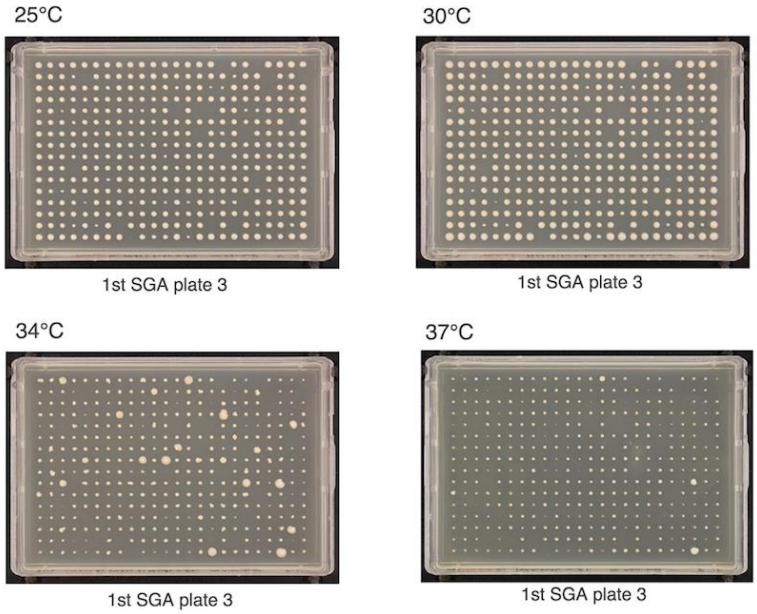

Figure 2.3 Validation of the double mutant selection. Double mutants from *zas1-Ts34* SGA were isolated at 25°C, 30°C, 34°C and 37°C respectively. Plate 3 was presented as an example. Severe growth defect of strains at restrictive temperatures (34°C and 37°C) indicates the temperature sensitive phenotype acquired from the *zas1-Ts34* allele.

In Figure 2.3, plate 3 was taken out from 9 experimental plates with *zas1-Ts34* double mutants as an example. As it shows, in the *zas1-Ts34* SGA, most double mutants form well-grown colonies at 25 °C and 30°C. However, at 34°C and 37°C, most double mutants did not grow into colony with normal size, and this trend is more severe at 37°C. This indicates that the series of selections are effective by which have eliminated contaminated species and isolated the double mutants as expected.

2.1.5 Results of the first round of SGA

Data analysis of *zas1-Ts34* SGA was performed as described in 2.1.3. Candidate genes with negative interaction cores below –0.15 are listed in Table 2.1.

Table 2.1 Candidate genes with genetic interaction with zas1 in zas1ts34SGA at 30°C

Systematic ID	Gene Name	Interaction value
SPAC26F1.04c	etr1	-0.599557399
SPCC970.07c	raf2	-0.507976628
SPAC22H12.02	tfg3	-0.494525465
SPBC1604.02c	ppr1	-0.489390855
SPBC13G1.08c	ash2	-0.479077401
SPBC6B1.04	mde4	-0.452329222
SPAC3G9.07c	hos2	-0.441808255
SPAC19A8.11c	irc6	-0.436936783
SPBC2D10.16	mhf1	-0.434322939
SPAC22E12.19	snt1	-0.426546332
SPBC15D4.10c	amo1	-0.422179489
SPBC21C3.02c	dep1	-0.420179231
SPAC11E3.03	csm1	-0.419905788
SPAC227.18	lys3	-0.380711609
SPAC1F7.01c	spt6	-0.344475797
SPBC17D11.04c	nto1	-0.34341478
SPAC22E12.11c	set3	-0.335134503
SPBC16G5.13	ptf2	-0.332556227
SPBC1685.08	cti6	-0.317225929
SPCC970.10c	brl2	-0.315988311
SPAC17G8.13c	mst2	-0.309688349
SPAC6B12.08	mug185	-0.305156425
SPAC22H10.07	scd2	-0.303771913
SPAC6G9.10c	sen1	-0.289798445
SPAC3H1.12c	snt2	-0.28660777

SPAC23D3.09	arp42	-0.276109722
SPBC405.06	xdj1	-0.243728596
SPAC3G9.04	ssu72	-0.227941731
SPCC18B5.03	wee1	-0.226376032
SPAC23C4.06c	efm6	-0.225386345
SPCC594.05c	spf1	-0.222954042
SPBC428.08c	clr4	-0.218500289
SPBP8B7.11	nxt3	-0.215612308
SPAC3G9.08	png1	-0.213216235
SPBC354.03	swd3	-0.211362203
SPBC3B9.11c	ctf1	-0.193724721
SPCC306.04c	set1	-0.192711636
SPBC21B10.09		-0.191349871
SPAC23H3.05c	swd1	-0.157598947

As the Bioneer V5 deletion library contains only non-essential gene mutants, to identify the positive interaction partner of *zas1* in genome wide including essential genes, multi-copy plasmid based suppressor screen (section 2.3) was performed in parallel. Besides, multiple spontaneous *zas1-Ts34* suppressors that lost the temperature sensitive phenotype have shown up during the pre-trials of the SGA (section 2.2). This has brought the concern on the validity of the positive interaction result from this SGA. Therefore analysis of negative interactions of *zas1* was the focus and positive interactions with *zas1* from SGA were not analyzed further. Later the multicopy suppressor screen has provided validated hits that interact with *zas1* positively (section 2.3).

With the non-essential genes that included in the haploid deletion library as the analysis background reference, I then performed gene ontology (GO) enrichment analysis for these negative interactions with AnGeli (Bähler 2015) and the result is listed in Table 2.2.

Table 2.2 GO term enrichment for zas1-Ts34 SGA

Genes with Enriched GO Terms	GO Terms	Frequency	Background frequency	p value
bdf2, snt1, spf1, set1, swd3, swd1	Heterochromatin assembly (GO: 0031507)	20.69 (6/29)	1.05 (36/3419)	0.0016
bdf2, sen1, lsc1, lsk1, prt1, ctf1, moc3, snt1, spf1, cti6, tho5, set1, swd3, swd1	Regulation of nucleobase-containing compound metabolic process (GO: 0019219)	48.28 (14/29)	11.85 (405/3419)	0.0022
sen1, lsc1, prt1, lsk1, moc3, snt1, spf1, cti6, tho5, set1, swd3, swd1	Regulation of DNA-templated transcription (GO: 0006355)	41.38 (12/29)	9.62 (329/3419)	0.0045
spf1, set1, swd3, swd1	Histone H3-K4 methylation (GO: 0051568)	13.79 (4/29)	0.50 (17/3419)	0.0059
nto1, snt1, spf1, cti6, set1, swd3, swd1	Histone modification (GO: 0016570)	24.14 (7/29)	2.95 (101/3419)	0.0067
sen1, lsc1, prt1, lsk1, moc3, snt1, spf1, cti6, tho5, set1, swd3, swd1	RNA biosynthetic process (GO: 0032774)	41.38 (12/29)	10.44 (357/3419)	0.0067
xdj1, SPBC543.02c, mug185, spf31	DnaJ domain (Pfam: PF00226)	13.79 (4/29)	0.56 (19/3419)	0.0067

Amongst the negative interactions, GO term analysis revealed an enrichment of genes involved in heterochromatin assembly, nucleic acid metabolism, transcription regulation, histone modification and RNA biosynthetic process. Since Zas1 has been reported to function as a zinc finger transcription factor (Okazaki & Niwa 2000b; Schiklenk et al. 2018), it is not surprising to find genetic interactions with genes that encode proteins acting in transcriptional regulation, which include genes with roles in histone modification and heterochromatin assembly. Further investigation is required to define in detail how zas1 is functionally linked to chromatin modification.

2.1.6 Second round of SGA

Previous experiments (Schiklenk et al. 2018) have suggested that the *cnd1* gene, which encodes a subunit of the condensin complex, is one of the transcriptional targets of Zas1. However, since uncoupling *cnd1* transcription from Zas1 control was insufficient to restore normal chromosome condensation, Zas1 might have a more direct role in mitotic chromosome condensation. To distinguish between genetic interactions with *zas1* that affect transcription globally from those that specifically affect condensin expression, a second round of SGA was designed as illustrated in Figures 2.1 and Figure 2.2B.

In order to uncouple the effect of Zas1 on condensin from general transcription regulation, the endogenous promoter of the *cnd1* condensin subunit was replaced by the promoter of the *cnd3* condensin subunit, which is not regulated by Zas1 (Schiklenk et al. 2018). Thus, the query strain for the second SGA contained the P_{cnd3}-*cnd1* construct tagged with the *hphMX6* selection marker in addition to the *zas1-Ts34* tagged with the *natMX6* selection marker.

Candidate mutants displaying negative interactions in the first SGA (Table 2.1) were selected for the second round of SGA. If any of these candidate genes were specific for the effect of *zas1* on condensin expression, then these should no longer display a negative interaction with the P_{cnd3}-*cnd1* strain. In contrast, genes that do not have a relationship with *cnd1* would still display negative interactions with zas1.

Deletion mutants corresponding to the candidate hits from the first SGA (Table 2.1) were inoculated freshly from the Bioneer V5 deletion library and crossed with either query strain 1 (*h⁻ zas1::zas1-Ts34-natMX6*) as SGA-a or query strain 2 (*h⁻ zas1::zas1-Ts34-natMX6* P_{cnd1}-*cnd1::hphMX6-*P_{cnd3}-*cnd1*) as SGA-b. For query strain 1, selection was performed as described for the first SGA (section 2.1.2). Since query strain 2 contained an extra selection marker, the selection procedure was adjusted (Haber et al. 2013; Braberg et al. 2014) accordingly to isolate triple mutants (Figure 2.2B): After the single mutant selection step by addition of geneticin and cycloheximide, another step of double mutants selection was conducted by adding Geneticin, clonNat and cycloheximide in the YE5S medium. With single mutants eliminated and competed growth between the double mutants and the triple mutants, the cell populations are

ready for the final triple mutant isolation by inclusion of three antibiotics (Geneticin, clonNat and Hygromycin) in YE5S media.

The corresponding control SGAs were conducted in parallel with control query strains 1 (h^- *ade6::ade6Δ-natMX6*) or control query strain 2 (h^- *ade6::ade6Δ-natMX6* P_{cnd1}-*cnd1::hphMX6-*P_{cnd3}-*cnd1*). The final selection step to isolate double/triple mutants was performed at 25°C, 30°C, 34°C and 37°C respectively. As in the first SGA, experiments at 34°C and 37°C were conducted to validate the haploid double/triple mutant selection steps. The results of the SGAs at 30°C are shown in Figure 2.4.

Since it is not possible to gain haploid double mutant from depletions of the same gene replaced by different selection markers, this linkage control can be set to assess the selection efficiency, as it should display synthetic lethal phenotype. Here strain h^+ *ade6::Δade6-kanMX6* was constructed and served as a linkage control in the experiment.

In the second round of SGA, 39 deletion mutants of candidate genes obtained from the first SGA (Table 2.1) together with the linkage control strain were distributed over four plates (Plate 1-4). To facilitate the assessment of reproducibility, each of these deletion mutants was represented 32 times by arraying each mutant covering two full columns on the 384 formatted agar plates (Figure 2.4).

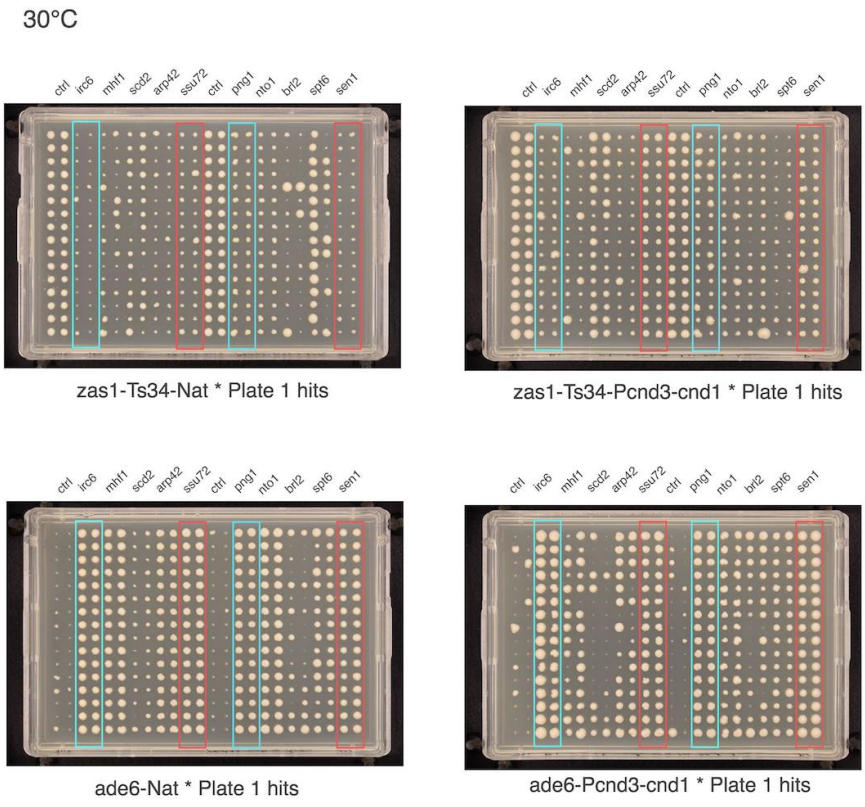

30°C

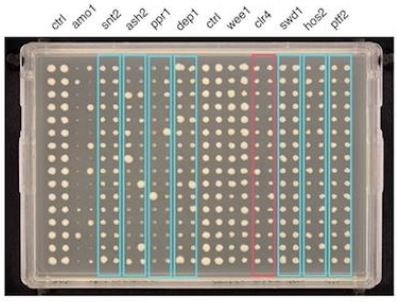

zas1-Ts34-Nat * Plate 2 hits

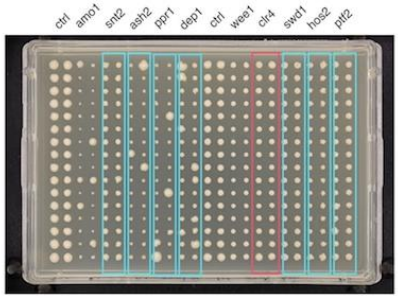

zas1-Ts34-Pcnd3-cnd1 * Plate 2 hits

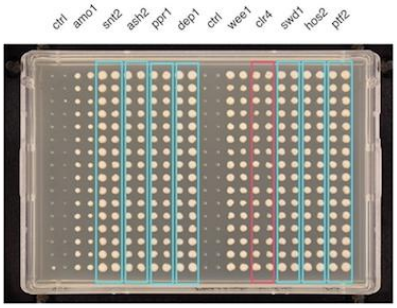

ade6-Nat * Plate 2 hits

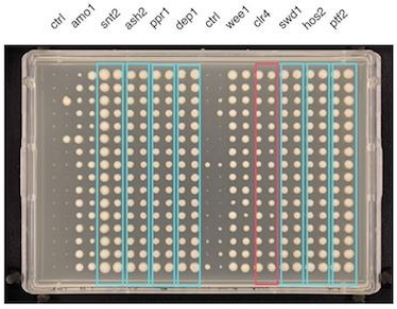

ade6-Pcnd3-cnd1 * Plate 2 hits

30°C

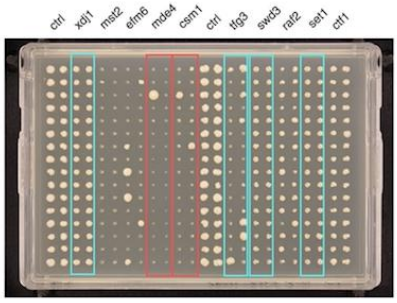

zas1-Ts34-Nat * Plate 3 hits

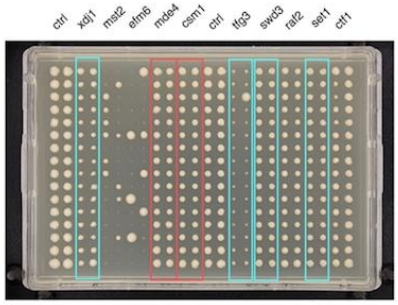

zas1-Ts34-Pcnd3-cnd1 * Plate 3 hits

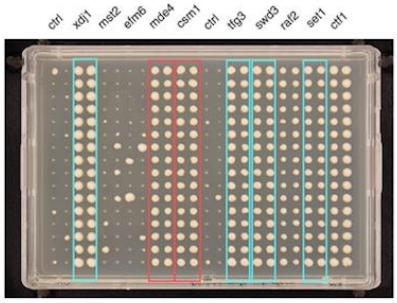

ade6-Nat * Plate 3 hits

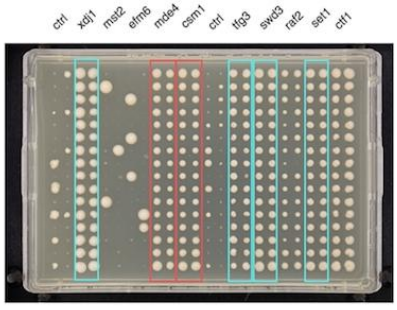

ade6-Pcnd3-cnd1 * Plate 3 hits

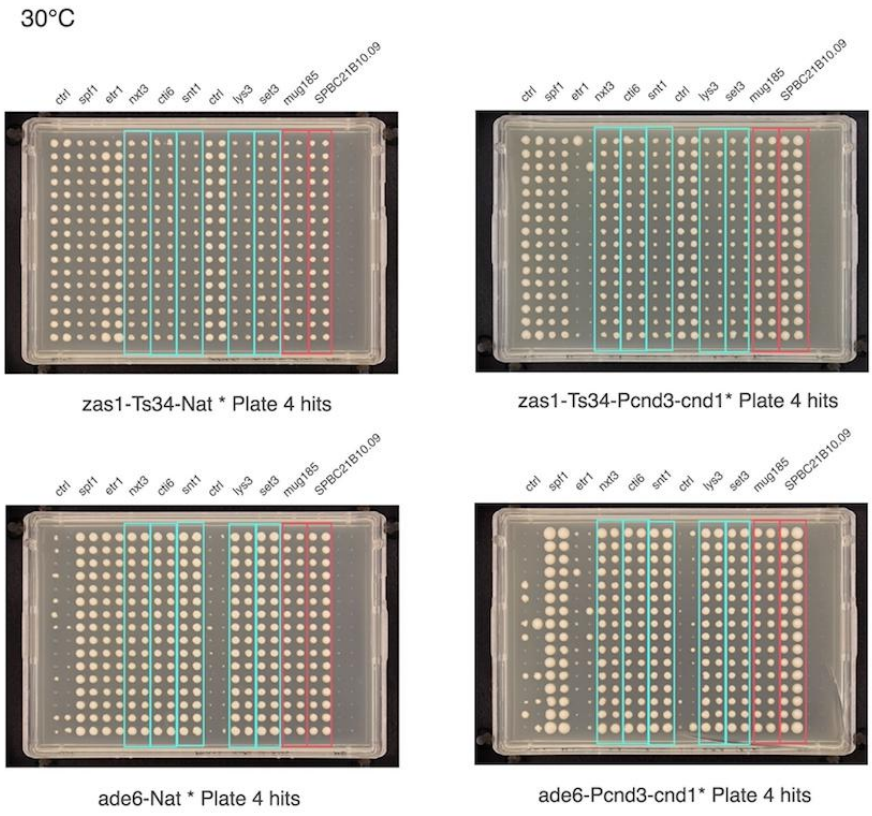

Figure 2.4 Evaluation of genetic interaction of candidate genes with *zas1* and their functional relationship with *cnd1*. Results of the second round of SGA at 30°C are presented. The subset of deletion library composed of candidate deletion mutants and linkage control (first two column on each plate, control) were arrayed as two columns for each strain and distributed on 4 plates (Plate 1-4). These candidate mutants arrays were crossed with two query strains (*zas1-Ts34-natMX6* (query strain 1, SGA-a) and *zas1-Ts34-natMX6-hphMX6-Pcnd3-cnd1* (query strain 2, SGA-b)) and two control query strains (h^- *ade6Δ-natMX6* (control query 1, SGA-a) and h^- *ade6Δ-natMX6-hphMX6-Pcnd3-cnd1* (control query 2, SGA-b)) respectively and underwent sequential meiosis, sporulation and selections. For each 4-plates graph, the left two plates show the results of the SGA-a and the right two display the results from the SGA-b. Deletion of genes that show synthetic sickness/lethality (SSL) with *zas1-Ts34* in both SGA-a and SGA-b are boxed in cyan. Deletions that display SSL in SGA-a with *zas1-Ts34* whilst the SSL phenotype has been significantly alleviated in SGA-b were boxed in red.

2.1.7 Results of the second round of SGA

Comparing to SGA-a with zas1-Ts34 query, if triple mutants obtained in SGA-b with query strain 2 *zas1-Ts34-*P_{cnd3}*-cnd1* have lost the synthetic lethal phenotype, the corresponding depleted genes are likely to negatively interact with zas1 through the connection with cnd1. Colonies of these hits are highlighted in red box in Figure 2.4 and summarized in Table 2.3. On the contrary, negative interactive genes that show similar synthetic lethality in both SGA-a and SGA-b are the ones not involved in the *cnd1* related network. They are boxed in cyan in Figure 2.4 and listed in Table 2.4.

Table 2.3. Genes displaying genetic interactions only in SGA-a

Gene ID	Gene Name	Product description
SPBC428.08c	clr4	Histone H3 lysine methyltransferase Clr4
SPAC11E3.03	csm1	Microtubule-site clamp monopolin complex subunit Csm1/Pcs1
SPBC6B1.04	mde4	Microtubule-site clamp monopolin complex subunit Mde4
SPAC6B12.08	mug185	DNAJ domain protein Mug185 (predicted)
SPBC21B10.09		Endomembrane system acetyl-CoA transmembrane transporter (predicted)

Table 2.4. Genes displaying genetic interactions in both SGA-a and SGA-b

Gene ID	Gene Name	Product description
SPBC13G1.08c	ash2	Ash2-trithorax family protein
SPBC1685.08	cti6	Histone deacetylase complex ubiquitin-like protein ligase subunit Cti6
SPBC21C3.02c	dep1	Sds3-like family protein Dep1
SPAC3G9.07c	hos2	Histone deacetylase (class I) Hos2
SPAC19A8.11c	irc6	Clathrin coat adaptor Irc6
SPAC227.18	lys3	Saccharopine dehydrogenase Lys3
SPBP8B7.11	nxt3	Ubiquitin protease cofactor Nxt3 (predicted)
SPAC3G9.08	png1	ING family homolog Png1
SPBC1604.02c	ppr1	Mitochondrial PPR repeat protein Ppr1
SPBC16G5.13	ptf2	Mst2 histone acetytransferase acytyltransferase complex subunit
SPCC306.04c	set1	Histone lysine methyltransferase Set1
SPAC22E12.11c	set3	Histone lysine methyltransferase Set3
SPAC22E12.19	snt1	Set3 complex subunit Snt1
SPAC3H1.12c	snt2	Lid2 complex PHD finger subunit Snt2
SPAC23H3.05c	swd1	Set1C complex subunit Swd1
SPBC354.03	swd3	WD repeat protein Swd3
SPAC22H12.02	tfg3	TFIID, TFIIF, Ino80, SWI/SNF, and NuA3 complex subunit Tfg3
SPBC405.06	xdj1	DNAJ protein Xdj1 (predicted)

Other candidates either did not show significant synthetic sick/lethal phenotype in neither of SGA-a and SGA-b or contain fitness issue even in the control query strain.

The hits from Tables 2.3 and 2.4 were analyzed for GO term enrichment respectively applying non-essential gene deletions in Bioneer V5 as analysis background (Tables 2.5 and 2.6).

Table 2.5. GO term enrichment of zas1 genetic interactive genes associated with cnd1

Genes with Enriched GO Terms	GO Terms	Frequency	Background frequency	p value
csm1, clr4, mde4	Abnormal kinetochore organization (FYP: 0000807)	60 (3/5)	0.20 (7/3419)	7.90E-05
csm1, clr4, mde4	Normal protein localization to centromere (FYP: 0002574)	60 (3/5)	0.67 (23/3419)	0.0034
csm1, mde4	Delayed onset of mitotic spindle elongation (FYP: 0002636)	40 (2/5)	0.088 (3/3419)	0.0058
csm1 clr4	Merotelic kinetochore attachment during mitosis (FYP: 0004381)	40 (2/5)	0.12 (4/3419)	0.0084

Amongst the 39 candidate genes from the first SGA analysis, 4 genes lost the synthetic phenotype in the second round of SGA: *clr4*, *mde4*, *csm1* and *mug185*, suggesting that their negative interactions with *zas1* are in the same network as *cnd1*. This list of hits, although without many genes, showed strong functional enrichment in AnGeli (Table 5) for GO categories associated with kinetochore organzation, protein localization to centromere, onset of mitotic spindle elongation and metotelic kinetochore attachment during mitosis. Specifically, csm1 encodes protein Csm1 (Synonyms: Pcs1) as microtubule-site clamp monopolin complex subunit (Rabitsch et al. 2003). Forming complex with Csm1, Mde4 encoded by mde4 is another subunit of microtubule-site clamp monopolin complex. Localising at the central core of centromere on fission yeast chromosomes, the Csm1/Mde4 complex clamp microtubule binding sites together to prevent merotelic attachment of kinetochores (Gregan et al. 2007). Although with our great interest for further investigation, it has been reported that in fission yeast, Csm1/Mde4 complex recruited condensin to kinetochores (Tada et al. 2011). The report showed physical interaction between Csm1 and Cnd1, Cnd2 and Cut3, all of which are subunit of condensin complex. Mde4 has been shown to physically interact with Cnd1 as well. Besides, csm1 also displayed negative genetic interaction with cut3. Thus the connections between csm1/mde4 and cnd1 showed in our SGA screen have been confirmed.

Gene clr4 encodes histone modification enzyme Clr4 that transfer methyl groups to lysine residue on histone proteins. Clr4 specifically targets histone 3 lysine 9 (H3K9) to mark the heterochromatin assembly (Rea et al. 2000). From a cross-species genetic interactomes study, *clr4* has been shown to genetically interact with *cut3* and *cut14* (Ryan et al. 2012). As the integrity of the centromeric heterochromatin structure is critical for the reliable clamping of chromosomes by kinetochores as reported (Gregan et al. 2007), the genetic interaction of *clr4* with condensin subunits could be readily explained by the connection of the Csm1/Mde4 and condensin.

The *mug185* gene has been predicted to encode a DnaJ-domain protein (Pombase) Mug185. DnaJ domain protein, also known as J-protein, is a member of Hsp40 molecular chaperones. It interacts with Hsp70 heat shock protein and activate its ATPase activity (Qiu et al. 2006). Further investigation is required to understand the genetic interaction between *mug185* and *zas1*.

Table 2.6 GO term enrichment of zas1 genetic interactive genes not involved in cnd1 related network

Genes with Enriched GO Terms	GO Terms	Frequency	Background frequency	p value
hos2, ptf2, set3, dep1, snt1, cti6, set1, ash2, swd3, png1, swd1, snt2	Histone modification (GO: 0016570)	66.67 (12/18)	2.95 (101/3419)	1.65E-11
hos2 ptf2 set3 dep1 snt1 cti6 tfg3 set1 ash2 swd3 png1 swd1 snt2	Chromatin modification (GO: 0016568)	72.22 (13/18)	6.17 (211/3419)	2.06E-09
hos2, set3, snt1, set1, ash2, swd3, swd1	Heterochromatin assembly involved in chromatin silencing (GO: 0070689)	38.89 (7/18)	0.53 (18/3419)	2.06E-09
hos2, set3, snt1, set1, ash2, swd3, swd1	Chromatin organization involved in regulation of transcription (GO: 0034401)	38.89 (7/18)	0.79 (27/3419)	2.80E-08
hos2, set3, dep1, snt1, cti6, tfg3, set1, ash2, swd3, png1, swd1, snt2	Regulation of DNA-templated transcription (GO: 0006355)	66.67 (12/18)	9.62 (329/3419)	3.42E-06
hos2, set3, dep1, snt1, cti6, tfg3, set1, ash2, swd3, png1, swd1, snt2	Regulation of RNA biosynthetic process (GO: 2001141)	66.67 (12/18)	9.62 (329/3419)	3.42E-06
hos2, ptf2, set3, dep1, nxt3, snt1, cti6, set1, ash2, swd3, png1, swd1, snt2	Cellular protein modification process (GO: 0006464)	72.22 (13/18)	13.48 (461/3419)	6.57E-06
set3, set1, ash2, swd3, swd1	Histone lysine methylation (GO: 0034968)	27.78 (5/18)	0.91 (31/3419)	5.88E-05
set3 cti6 snt2	PHD finger (Pfam: PF00628)	16.67 (3/18)	0.29 (10/3419)	0.0016

Candidate genes for which the genetic interaction with *zas1* was not influenced by uncoupling *cnd1* expression are enriched in GO terms for the processes of histone modification, heterochromatin assembly, transcription regulation and RNA biosynthetic regulation. Zas1 may relate to the process of inactivation of transcription through chromatin modification. The enriched PHD (plant homeodomain) finger domain in the candidates Set3, Cti6 and Snt2, which recognizes H3K9 methylation (Sanchez & Zhou 2011; Roguev et al. 2003), furthermore supports an involvement of Zas1 in gene silencing. These connections are consistent with the findings that transcription is down-regulated before mitosis and that C_2H_2 zinc finger transcription factors are coordinately inactivated at this point of the cell cycle (Katherine et al. 2017; Dovat et al. 2002).

2.2 Spontaneous suppressors of zas1 mutants

Among the population of *zas1-Ts34* with the background of lab wild type strain 972h$^-$, it has been noted during the project that substantial number of spontaneous suppressors of zas1 ^{ts} mutant appeared. For example, a serial dilution test of five individual colonies of the *zas1Ts34* strain revealed that three clones spontaneously lost their temperature sensitive phenotype at the restrictive temperature of 34°C (Figure 2.5). The high rate of reversal of the ts phenotype cannot be explained by random mutation, since it is significantly higher than the natural mutation rate in the *S. pombe* population, which has been estimated at 2×10^{-10} mutations per site per generation (Farlow et al. 2015). During the course of the project, ten spontaneous suppressors were collected in total and labelled as spontaneous mutant SM_1 to SM_10. In contrast, *zas1-Ts34* mutant strains with a PEM-2 background had never gained spontaneous suppressors of the temperature-sensitive phenotype.

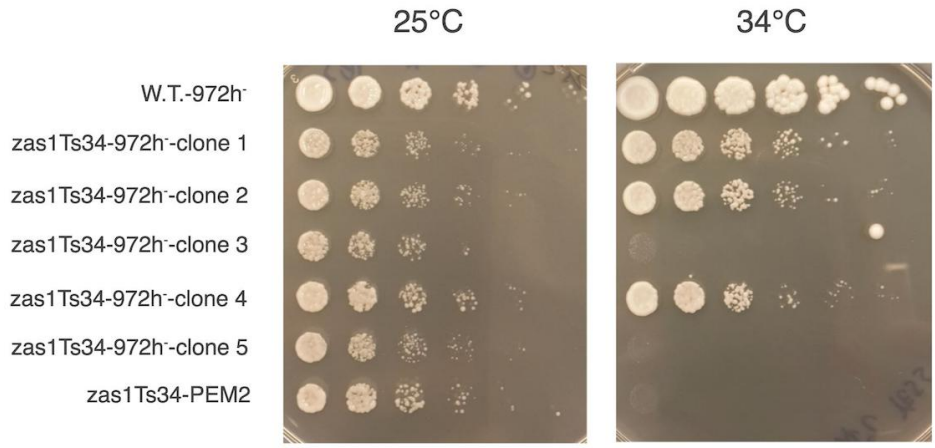

Figure 2.5 Growth test of *zas1Ts34*-972h$^-$ clones and PEM-2 strain with *zas1-Ts34*. Exponentially grown cell cultures of 972h- wild type haploid, 5 clones of *zas1-Ts34*-972h$^-$ and PEM2-*zas1Ts34* strain were spotted onto YE5S media in a 5-fold dilution and incubated at 25 °C and 34 °C for 3 days respectively. Clone1, 2 and 4 of *zas1Ts34*-972h$^-$ have lost the temperature sensitivity feature of zas1-Ts34 mutation.

To understand the basic physiology of the zas1-Ts34 temperature sensitivity in both 972h$^-$ and PEM-2 backgrounds, flow cytometry analysis was applied to measure their DNA content. An unsynchronized fission yeast haploid population should display a predominant 2C DNA content peak since most cells spend most time in G2 phase of the cell cycle. Unsynchronized diploid cells consequently display a prominent 4C peak (Noguchi & Forsburg 2009).

FACS analysis of unsynchronized *zas1* mutants showed, surprisingly, that most *zas1-Ts34* 972h$^-$ strains that remained temperature sensitive displayed, in addition to a small 2C peak, a prominent DNA content peak at 4C, which is similar to wild-type diploid cells (Figure 2.6A). By contrast, *zas1-Ts34 PEM-2* cells only displayed a 2C DNA peak, similar to haploid wild-type cells (Figure 2.6B). Interestingly, all but one spontaneous suppressor clones of *zas1-Ts34* 972h$^-$ also displayed only a 2C DNA content (Figure 2.6C). DNA sequencing of the *zas1* genes in these spontaneous suppressors revealed no additional mutations in the gene.

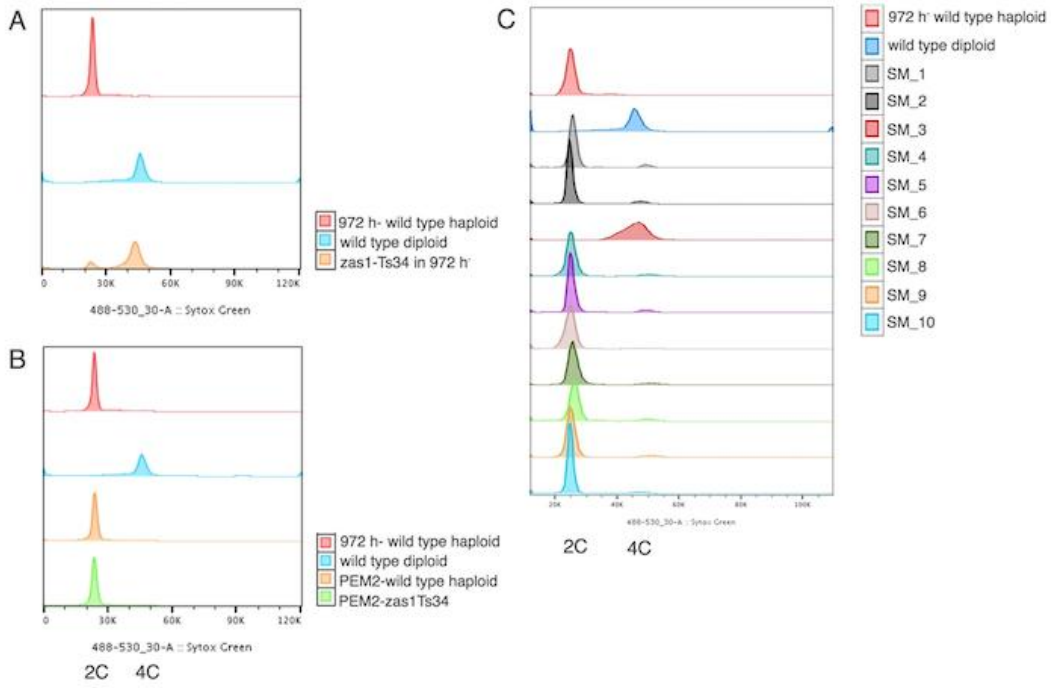

Figure 2.6 Flow cytometry analysis of DNA content in asynchronous cell cultures with fixation and stained with Sytox Green. (A) Profiles of wild type 972h- haploid, wild type diploid and zas1-Ts34 in 972 h$^-$ background. A single peak corresponding to 2C DNA content or 4C DNA content is shown in 972h- haploid or diploid wild type strain. zas1-Ts34-972h$^-$ has aberrant two peaks DNA distribution with large populations of cells have 4C DNA content as diploid. (B) DNA content profiles of 972h- haploid, diploid, PEM2-wild type and PEM2-zas1Ts34 strain. Both PEM2-wild type and PEM2-zas1Ts34 have single peak corresponding to 2C DNA content as 972h$^-$ wild type haploid. (C) DNA content profiles of spontaneous suppressors of zas1-Ts34-972h$^-$ and wild type haploid/diploid. Out of 10 spontaneous suppressors (SM_1~SM_10) of zas1-Ts34-972h- that lost temperature lethal phenotype, nine strains (except SM_3) display single peak corresponding to 2C DNA content as wild type 972h$^-$ strain.

The unique feature of the PEM-2 strain is the presence of a recessive cycloheximide resistance marker and a cycloheximide-sensitive allele in the h$^-$ mating type locus. In addition, the strains contains an *smt0* mutation in the h$^-$ mating type locus to prevent mating type change (Styrkfirsdttir et al. 1993).

As cells did not undergo cycloheximide selection, the lack of spontaneous suppressors in the PEM-2 strain can presumably be explained by the *smt0* mutation. The hypothesis is that as *zas1* is essential for cell growth, *S. Pombe* would attempt different strategies to maintain its survival when the function of zas1 is impaired. It either tries to become diploid with duplicated DNA, by which the impaired function could be compensated by the additional DNA or perhaps additional copy of cell machinery. And to increase the survival rate, diploid can easily become spores and enter the dormant status G0. Or as Zas1 is a transcription factor and it regulates expression of many essential genes, cells can overcome the sickness by correcting the transcriptional regulation defect caused by impaired Zas1. To this end, cell can harness and mutate other protein involved in the transcription but still keep the cell as haploid. This scenario could correspond to the case of haploid spontaneous suppressor we have encountered.

To prevent the accumulation of spontaneous suppressors and to maintain genetically stable haploid *zas1-Ts34* cells, all further strains in this thesis were constructed in the PEM-2 background.

2.3 *Zas1* multi-copy suppressor screen

2.3.1 Outline of the suppressor screen

To identify the physical interaction partner or genes acting in the same genetic pathway as *zas1*, a multi-copy suppressor screen with a plasmid-based genomic library was designed. The *S. pombe* genomic library was a kind gift from Dr. Charles Hoffman. The library had been constructed with DNA fragments from fission yeast strain KGP5 (Wang et al. 2005) cloned into vector pEA500 (Apolinario et al. 1993), which contains the *his7*$^{+}$ selective marker. 70% of the plasmids contained DNA inserts with an average insert size of 3.9 kb (Figure 2.7). As the gene density in the *S. Pombe* genome corresponds to one gene every ~2.5 kb and the average length of all genes across the genome is 1.4 kb (Wood & Nurse 2002), this genomic library is considered eligible to provide plasmids holding a large fraction of intact protein-coding fission yeast genes.

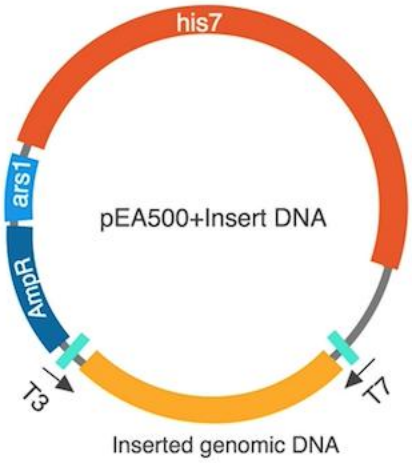

Figure 2.7 Representation of the genomic library plasmid based on pEA500 vector. pEA500 vector contains *his7*$^{+}$ as the selectable marker. The insert DNA was generated from genomic DNA from KGP5 strain and filled in the vector between T3 and T7 sequence. 70% of insert DNA have average size of 3.9 kb.

The genomic library was amplified in DH5-alpha *E. coli* cells. To avoid any ploidy instability issue (see section 2.2), *zas1-Ts34 PEM-2* cells were crossed with strain FWP60 (*his7-366*) to generate the host strain FWP60 *zas1-Ts34 PEM-2* (*his7⁻)* (abbreviated as FP *zas1-Ts34*) for the suppressor screen. To identify multicopy suppressors that be able to alleviate the temperature lethal phenotype conferred by the *zas1-Ts34* allele (Figure 2.8), the host strain *FPzas1-Ts34* was transformed to his7⁺ with the genomic library plasmids via the LiAc/TE method and plated onto 100mm x 15mm plates with selective EMM4S (without histidine) media agar. After incubation at 25°C for 6 days, about 42,000 clones formed. With an average insert size of 3.9 kb, this number theoretically covers 12-times of the fission yeast genome. Clones were replicated onto a new batch of selective EMM4S (without histidine) agar plates and incubated at 34°C for 6 days to select for suppressors of the temperature-sensitive phenotype.

This resulted in 48 clones that supported growth at the restrictive temperature of 34°C. To validate that the suppression of the ts phenotype is indeed conferred by the plasmids, plasmids from these clones were isolated and amplified in DH5-alpha *E. coli* cells and used to transform host strain FP *zas1-Ts34*. The new transformants were obtained at 25°C and then shifted to 34°C for 6 days. Only 9 clones were able to proliferate at the restrictive temperature. Plasmids were again isolated, amplified in DH5-alpha *E. coli* cells and subjected to DNA sequencing using the vector-specific primers T3 and T7 to sequence both ends of the inserts. Vector pEA500 served as a negative control throughout these experiments.

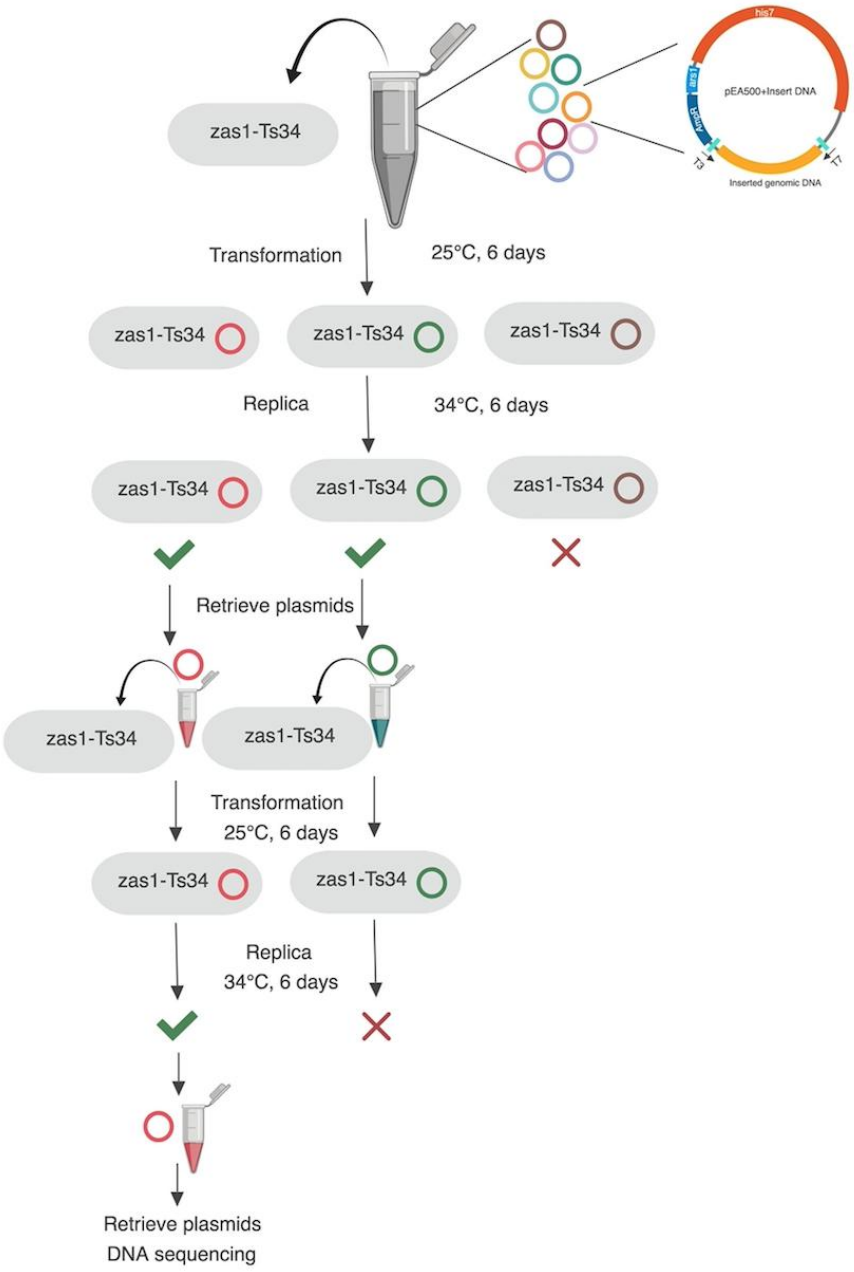

Figure 2.8 Procedure of multicopy suppressor screen. Plasmid-based S. pombe genomic DNA library was transformed into the host strain with *zas1-Ts34* mutation (FWP60-PEM2-*zas1-Ts34*). Transformants formed at 25°C were replicated and incubated at 34°C for suppressor isolation. Retrieving and re-transforming the corresponding plasmids validated the rescuing of the temperature sensitive phenotype. DNA sequence of the genomic fragment contained in the plasmids was sequenced.

2.3.2 Analysis and validation of multi-copy suppressors

Out of the 9 candidate plasmids (Table 2.7), three contained the *zas1* gene, which confirmed the validity of the screen. Two plasmids contained the *klf1* gene. Like Zas1, Klf1 is a C_2H_2 zinc finger transcription factor and has been reported to physically interact with Zas1 at G0 but not vegetative phase (Shimanuki et al. 2013). The remaining four plasmids contained the *usp101* gene, which encodes the protein Usp101 as the essential part of U1 snRNP that initiate the splicing process in fission yeast.

In the initial validation experiment shown in Figure 2.9, strains with these plasmids were streaked onto –histidine selective media and incubated at the permissive temperature of 25°C or the restrictive temperature of 34°C, respectively. The empty vector pEA500 was used as a negative control. With the exception of one *usp101* clone (*usp101-c17*), all *zas1*, *klf1* or *usp101* plasmids indeed rescued the temperature-sensitive phenotype of the FP *zas1-Ts34* mutant at 34°C.

Table 2.7. Rescuers identified from multicopy suppression screen

Gene Name	Gene ID	No. of clones	Annotation
zas1	SPBC1198.04c	3	transcription regulator Zas1
klf1	SPAC1039.05c	2	C_2H_2 zinc finger transcription factor Klf1
usp101	SPAC19A8.13	4	U1 snRNP-associated protein Usp101

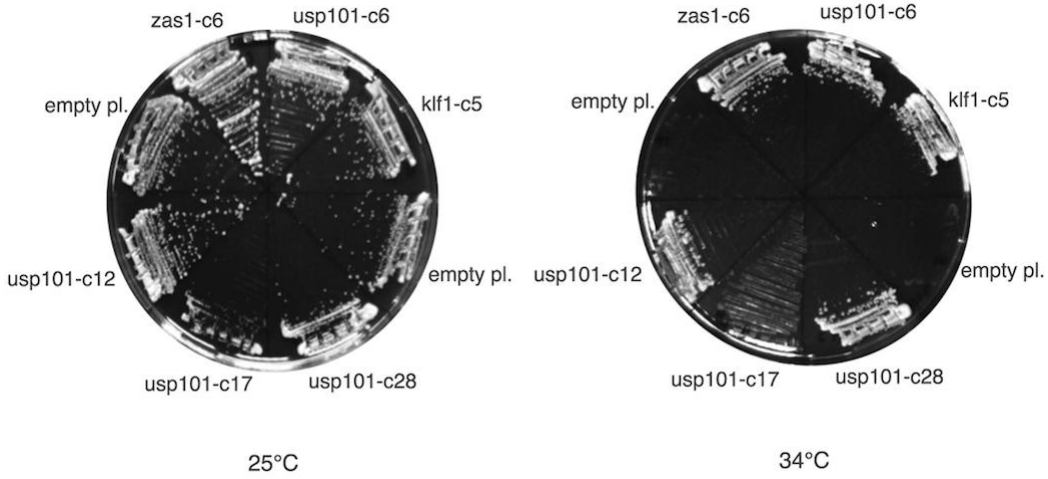

Figure 2.9 Multicopy suppression of *zas1-Ts34* mutation by overexpression of *zas1, klf1* or *usp101*. His+ transformants of FWP60-PEM2-*zas1-Ts34* harboring either pEA500 empty vector (empty pl.) or *zas1* (*zas1*-c6), *klf1* (*klf1*-c5), *usp101* (*usp101*-c6, c12, c17 and c28) were plated onto EMM4S (no histidine) media and incubated at 25°C and 34°C respectively for 3 days.

The suppression indicates that over-expression of Usp101 can compensate the consequence of functional impairment of Zas1. This could be attribute to two possibilities. The first is that Usp101 may work in the same pathway as Zas1, playing roles either in its downstream or upstream. Or there may be physical interaction between Zas1 and Usp101. To distinguish these two possibilities, we firstly turned back to the raw data of previous ChIP-seq experiment from Christoph Schiklenk to whether the *usp101* gene might be a target of Zas1 transcription factor binding. Remarkably, this identified a significant binding peak of Zas1 at the promoter of *usp101* (Figure 2.10), although although the peak height was not ranked high in the previous analysis (Schiklenk et al. 2018).

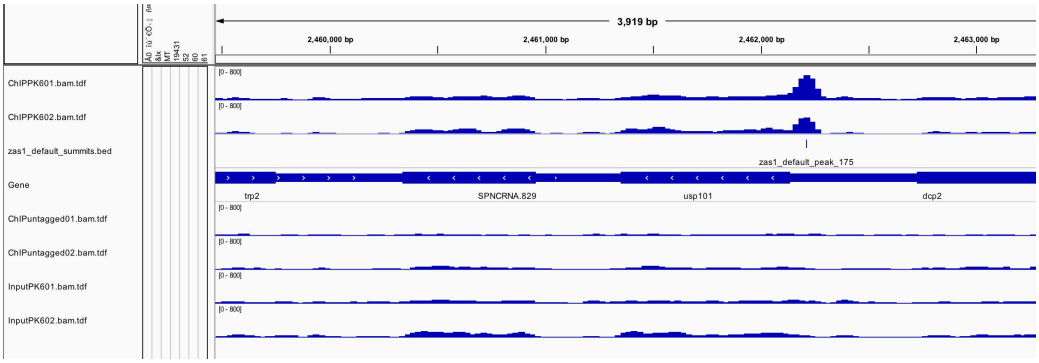

Figure 2.10 ChIP-seq profiles at the gene *usp101* loci of strain Zas1-PK$_6$ and untagged strain as control. The profile has generated from two independent experiments. The y-axis represents the amount of reads. A significant binding peak of Zas1 was located at the promoter region of *usp101* in the strains expressing Zas1-PK$_6$.

To test the hypothesis that *usp101* transcription is controlled by Zas1, the Usp101 protein levels were compared between wild-type and *zas1-Ts34* mutant cells, both in the PEM-2 background.

For this, the PK$_3$ epitope tag was fused to the carboxyl terminus of Usp101, using *kanMX6* as a selection marker. Two independent clones of wild-type PEM-2 and *zas1-Ts34* PEM-2 cells were harvested at exponential growth at permissive temperature 25°C and processed for western blotting with the V5 antibody. Blotting against tubulin with the anti-TAT1 antibody served as a loading control. As it is shown in Figure 2.11, Usp101 protein levels were significantly reduced in *zas1-Ts34* mutant cells when compared to the wild-type control, which is consistent with the hypothesis that expression of *usp101* is regulated by Zas1.

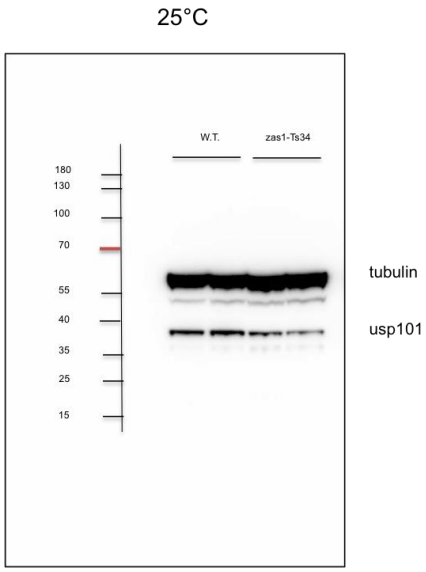

Figure 2.11 Protein expression of *usp101* is reduced in *zas1-Ts34* mutants at the permissive temperature. Western blotting of whole-cell extracts from asynchronous exponential grown cultures of wild type (PEM2-WT) and zas1-Ts34 mutant (PEM2-*zas1-Ts34)* at 25°C were performed to compare the protein level of Usp101 (30.2 kDa) against the fused PK_3 tag. Western blotting probed with anti-TAT antibody against α-tubulin served as loading control. Results of two independent experiments are shown.

2.3.3 Transcriptome profiling in zas1 mutants

As described in section 1.4, *usp101* encodes the protein Usp101 as the homolog of U1-70K in mammalian cells and 43% of protein coding genome in *S. pombe* contains intron, if Usp101 is indeed a key target of the Zas1 transcription factor and the reduction of Usp101 was responsible for the temperature-sensitive phenotype of the *zas1-Ts34* mutant, I would expect that the splicing process would be largely skewed in *zas1-Ts34* mutants at the restrictive temperature.

To test this hypothesis, RNA-seq was applied to map the transcriptome profile of PEM-2 wild-type and PEM2-*zas1-Ts34* mutant cells, as well as a PEM2-*zas1-Ts34* mutant strain overexpressing *usp101* before and after the promoter induction at 25°C or 34°C respectively. A PEM-2 *zas1-Ts34* mutant strain with empty vector was used as negative control in these experiments (Figure 2.12).

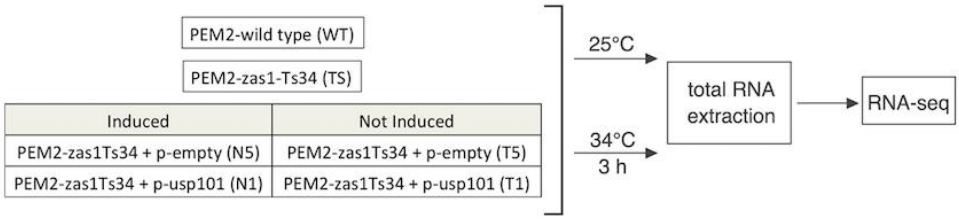

Figure 2.12 Procedure of transcriptome profiling experiment.
PEM2-wilde type (WT), PEM2-zas1Ts34 (TS) in EMM5S media and TS strains with multicopy plasmids carrying either empty vector or usp101 in selective media with/without thiamine (T5, N5, T1, N1) were grown exponentially at 25°C and 34°C for 3h. Samples were collected via snap freezing and total RNA was extracted for transcriptome profile mapping.

To overexpress Usp101, vector REPNTAP (Tasto et al. 2001) with a *LEU2* selective marker was used. Usp101 was tagged at the its N terminus with a TAP tag that was placed under the inducible promoter P_{nmt81}. The nmt (no information with thiamine) promoter can be repressed by thiamine addition to the growth media or induced by removal of thiamine, respectively. There are three versions of nmt promoter ranked by strength. With ATATAAA deleted from the original nmt1 sequence, nmt81 promoter has the weakest strength in driving gene expression, with 1.2±0.3 times of expression under repressed condition comparing to the wild type whilst 7.2±2 times of expression upon induction (Forsburg 1993; Basi et al. 1993). 16-18 hours incubation in the thiamine free

growth media is required to activate the nmt promoter (Převorovský et al. 2015; Maundrell 1990).

PEM-2 wild-type (WT) and PEM2-*zas1Ts34* (TS) strains were incubated in EMM5S media at 25°C. Half of the exponential cell cultures from each strain were separated into 34°C incubator for 3 h. Samples were taken and snap frozen from cell cultures at both 25°C and 34°C.

PEM-2 *zas1Ts34* strains harboring multi-copy overexpression plasmids were grown to exponential phase in selective media EMM4S (no leucine) with thiamine or without thiamine for 22 h and half of the cultures were then shifted to 34°C for 3h before taking samples from cultures both at 25°C and 34°C.

Total RNA was extracted from all samples and quality of RNA prep was confirmed before DNA library preparation and next generation sequencing at EMBL's GeneCore Facility. A ribosome depletion protocol rather than a polyA selection protocol was applied to prepare the library, since Usp101 has been reported to protect pre-mRNAs from polyadenylation (Kaida et al. 2010; Kaida 2016). After the rRNA depletion and RNA-seq library preparation steps, unidirectional sequencing was performed with Illumina sequencer NextSeq 500. About 500 million reads were generated with average size of 85 bases.

2.3.4 Evaluation of usp101 mRNA levels

First, the mRNA levels of *usp101* in all the experimental strains were examined. The results are summarized in Figure 2.13. Expression of *usp101* in PEM-2 *zas1-Ts34* mutant cells (TS) is significantly reduced when compared to PEM-2 wild type cells (WT). The difference is more prominent at 34°C. This is consistent with the reduction in Usp101 protein levels in the mutant cells and the conclusion that expression of *usp101* is regulated by the Zas1 transcription factor.

Under both, induced (N5) and uninduced (T5) conditions, the PEM-2 *zas1-Ts34* mutant strain with an empty vector showed similar mRNA levels of *usp101* comparing to the PEM-2 *zas1-Ts34* mutant cells without any plasmid (TS) (Figure 2.13). This confirms the minimized effect of empty plasmid to the expression of usp101.

Similarly usp101 mRNA levels were comparable between the PEM-2 *zas1-Ts34* mutant cells without plasmid (TS) and the PEM-2 *zas1-Ts34* mutant with the *usp101* overexpression plasmid under repressive conditions (T1). Whereas overexpression of *usp101* in thiamine-free media (N1), resulted in 15-18 times more usp101 mRNAs than in the TS control and 4-6 times more than the WT control. The over-expression of usp101 is more significant at 34°C than at 25°C. Thus it is confirmed that multicopy plasmids of usp101 have conferred overexpression of *usp101* in *zas1-Ts34* mutant under induced condition.

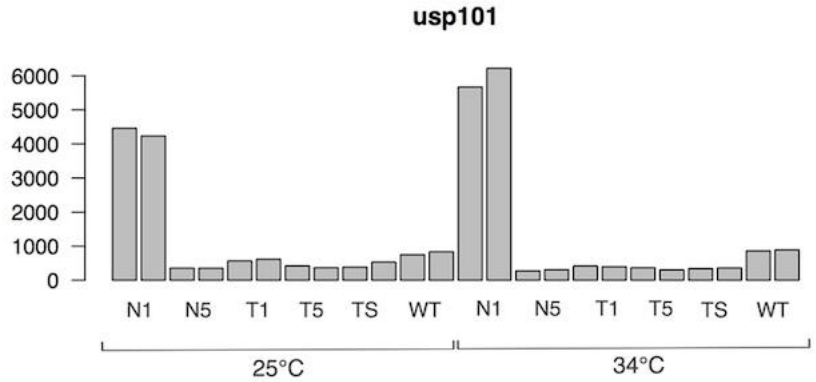

Figure 2.13 mRNA level of *usp101* is reduced in PEM2-*zas1-Ts34* mutant comparing to the PEM2-wild type at both 25°C and 34°C. Multicopy plasmid carrying *usp101* conferred overexpression of Usp101 in the *zas1-Ts34* mutant. mRNA levels of *usp101* obtained from RNA-seq experiment are shown. Results from two independent experiments are presented. N1: PEM2-*zas1-Ts34* mutant with Usp101 overexpression. N5: PEM2-*zas1-Ts34* holding multicopy plasmids of *usp101* but with nmt81 promoter repressed. T1: PEM-2 *zas1-Ts34* mutant harboring empty vector with nmt81 promoter activated. T5: PEM-2 *zas1-Ts34* mutant with empty vector with repressive nmt81 promoter.

2.3.5 Zas1 mutant cells display splicing defects

Having confirmed the *usp101* overexpression system, the genome-wide splicing status of these strains was further evaluated. Data analysis and data visualization were performed by Lin Gen, bioinformatician from Steinmetz lab in EMBL. For every strain, the number of reads for each intron was counted. If splicing defect existed in *zas1-Ts34* mutants (TS), intron reads should be higher than in wild-type cells (WT) and this defect should be rescued by *usp101* overexpression, i.e. the ratio of intron reads in WT to TS should be smaller than 1 (WT/TS<1) and the logarithm at base 2 of this ratio would be smaller than 0 (Log_2 (WT/TS)<0), which I define as ratio score *R*.

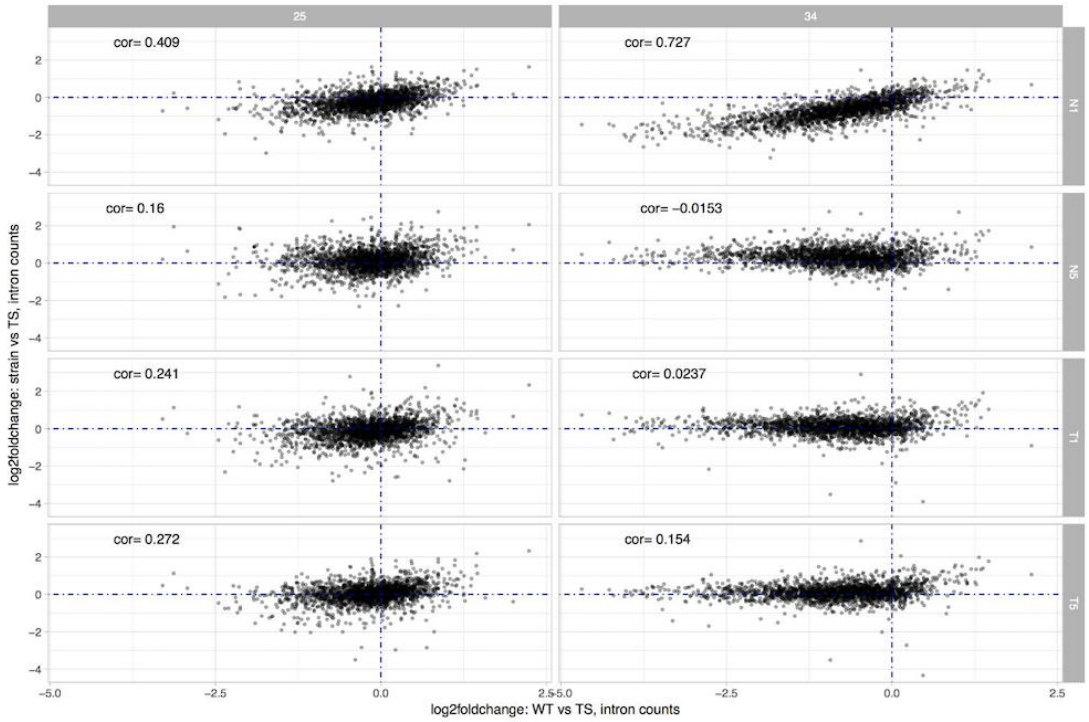

Figure 2.14 Genomic wide higher amount of intron reads were detected in the PEM2-*zas1-Ts34* mutant (TS) comparing to the PEM2-wild type (WT). The overall intron counts has recovered to be similar to the WT in the *zas1-Ts34* strain with usp101 overexpression especially at 34°C (N1, up-right plot). In the transcriptome profile map, each intron reads was counted for samples from strain PEM2-WT (WT), PEM2-*zas1-Ts34* (TS), PEM2-*zas1-Ts34* with empty vector (N5, T5) and PEM2-*zas1-Ts34* carrying multi-copy usp101 plasmid (N1, T1) under nmt81 promoter activated (N) or inactivated (T) conditions at 25°C and 34°C respectively. Comparison was generated by plotting the ratio of intron reads in N5, T5, N1, T1 to TS respectively against the ratio of WT to TS. The x-axis indicates the ratio R of intron reads in the WT to the TS. The y-axis represents the ratio of intron reads in each of the rest samples to the TS, including N5, T5, N1 and T1. Logarithm at base 2 was taken to present the calculated ratio. Results from 25°C and 34°C are listed in the first and second column respectively. Correlation of the two axis value was labelled in the up-left corner of each plot.

At the permissive temperature of 25°C, the ratio score *R* varied for different intron reads around the zero value (Figure 2.14, x-axis). At the restrictive temperature of 34°C, however, the distribution of the ratio scores *R* was consistently shifted towards negative values, i.e. the number of intron reads was increased in the mutant when compared to the wild-type strain at the restrictive temperature 34°C, consistent with a splicing defect in the mutant.

The ratio scores *R* were then used as a basis to plot the ratio between the four expression conditions (N1: *usp101* induced; T1: *usp101* repressed; N5: empty plasmid induced; T5: empty plasmid repressed) and the *zas1-Ts34* (TS) condition, which was defined as ratio score *E* (Figure 2.14, y-axis). Therefore, if one of the four expression conditions reverted the changes in intron counts caused by the *zas1-Ts34* mutation, a positive correlation between ratios *R* and *E* should become apparent, i.e. introns that are less abundant in WT than in TS cells (negative *R* score) should also be less abundant in the *usp101* overexpression strain than in TS cells (negative *E* score); introns that are more abundant in WT than in TS cells (positive R score) should also be more abundant in the *usp101* overexpression strain than in TS cells (positive *E* score) if *usp101* overexpression rescued any splicing defects. Such a correlation was indeed apparent when *usp101* was overexpressed from the plasmid (N1, top-right plot) in PEM2-zas1Ts34 at 34°C, but not if expression was repressed (T1) or in the case of the empty plasmid (N5, T5) (Figure 2.14). The similar trend can be found at 25°C as well but not prominent, which is consistent with the knowledge that 25°C is a permissive temperature for *zas1-Ts34* mutant. Thus this analysis demonstrates that the increase in intron reads across the genome in the PEM2-*zas1-Ts34* mutant can be reverted by *usp101* overexpression.

However, this increase in intron reads can either be explained by a splicing defect or an increase in the number of transcripts due to a general increase in gene expression. To distinguish between these two possibilities, reads that aligned within introns, spanned intron-exon and exon-exon junctions were defined as the total number of reads. Reads that could be only aligned fully in the intron region or that span the exon-intron boundaries were recognized as the unspliced reads.

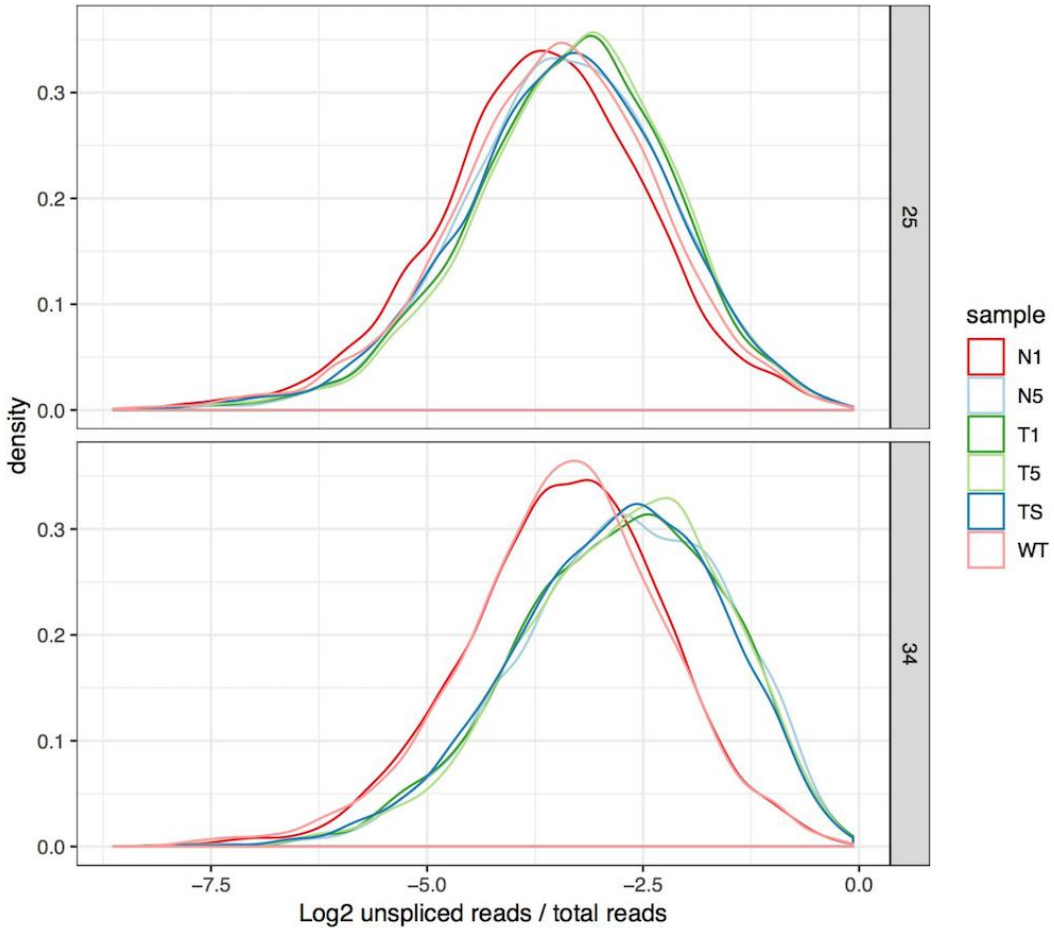

Figure 2.15 The splicing defect derived from the PEM2-*zas1-Ts34* mutation is rescued in the strain with Usp101 overexpression. For each intron sequence fragment, ratio of unspliced to the total reads was taken and the logarithm at the base of 2 was calculated for the presentation (x-axis). Histogram was plotted for the distribution of the measures of the unspliced/total reads ratio of all the introns across the protein coding genome, which represent the splicing states in a cell. The y-axis indicates the count of measures.

The splicing ratio *S* was defined by the $\log_2$ score of the ratio of unspliced reads to the total number of reads for each intron across the protein coding genome. As shown in Figure 2.15, the distribution of *S* values is shifted to larger values for the PEM2-*zas1-Ts34* mutant (TS) when compared to PEM2-wild-type (WT), indicating an increase in the fraction of unspliced reads, and this effect is more pronounced at the restrictive

temperature of 34°C than at 25°C. The same shift can be observed for the PEM2-*zas1-Ts34* mutant with empty vector under repressed or induced conditions (T5/N5) or with the *usp101* overexpression plasmid under repressed conditions (T1). Strikingly, for the strain harboring the *usp101* overexpression plasmid under induced conditions (N1), the distribution of *S* closely resembled that of PEM2-wild-type cells. This strongly suggests that the splicing defect caused by *zas1-Ts34* mutation has been rescued by the over-expression of *usp101*.

In conclusion, these results confirm the accumulation of unspliced precursor mRNA transcripts in the *zas1-Ts34* strain, most likely due to the reduction in *usp101* expression, which is transcriptionally regulated by the Zas1 transcription factor.

2.4 The reduction of Usp101 levels is responsible for the zas1-Ts34 mutant phenotype

Despite having been identified as a key transcription factor for genes essential for cell proliferation, including genes encoding the condensin subunit Cnd1 or the microtubule regulator Peg1, uncoupling the transcription of any of these target genes from Zas1 control failed to restore wild-type growth in *zas1* mutant cells (Schiklenk et al., 2018). Since *usp101* down-regulation in the *zas1-Ts34* mutant results in a general splicing defect as indicated, it might explain the temperature-sensitive phenotype of the mutant. If this hypothesis is correct, restoring Usp101 levels should rescue the lethal phenotype of the *zas1-Ts34* mutant at the restrictive temperature.

To test this idea, the growth phenotype of PEM2-*zas1-Ts34* mutant cells harboring plasmids for expression of *zas1*, *zas1-cDNA*, *usp101*, *cnd1*, *cnd1-cDNA* and *klf1* was assessed.

Wild type PEM-2 and PEM2-*zas1Ts34* with the empty vector were used as positive and negative controls, respectively. The plasmids were based on the pREP-NTAP vector, which can be used to express an N-terminally TAP-tagged gene of interest driven by the weak strength P_{nmt81} promoter. Genes of interest were amplified from genomic DNA of strain $972h^-$ and inserted into pREP-NTAP vector by Gibson assembly. All of strains were grown exponentially at 25°C in selective EMM4S (no leucine) media with or without thiamine for 22 h and then spotted in 5-fold serial dilutions onto selective media (EMM4S (no leucine)) with or without thiamine). The plates were incubated at 25°C, 30°C, 34°C or 37°C for 3 days respectively.

The results of the spotting assay are shown in Figure 2.16. As expected, the presence of *zas1*, either as genomic copy or as cDNA version, rescued the temperature-sensitive phenotype of *zas1-Ts34* at the restrictive temperatures of 34°C and 37°C, even when expressed at low levels under non-induced conditions. In accordance with the data from the multicopy suppressor screen, expression of *usp101* similarly rescued the ts phenotype at both restrictive temperatures and even when not induced by omitting thiamine from the media.

In contrast, overexpression of *cnd1*, either as genomic copy or as cDNA version, was unable to rescue the ts phenotype, consistent with previous observations (Schiklenk et al., 2018). This indicates that normal expression of Cnd1 protein itself is not sufficient to compensate the growth failure of zas1-Ts34 mutant. This observation lends further support to the results obtained from the transcriptome profiling indicating that the splicing process in the zas1-Ts34 mutant is impaired generally rather than only integrity of single gene is compromised.

Interestingly, expression of *klf*1, the heterodimer partner of Zas1 at G0, restored the zas1-Ts34 temperature-sensitive phenotype at 34°C but not at 37°C, which is consistent with the isolation of *klf1* clones in the suppressor screen (see 2.3.2). This suggests that Klf1 might be able to take over some but not all of the transcriptional control functions of Zas1.

It is noticeable here that all strains have shown similar growth phenotype at plates with and without thiamine. This indicates the leakage of the nmt81 promoter even in the repressive condition. It is reported that nmt81 promoter still be able to induce 1.2±0.3 times of endogenous expression when repressed (Forsburg 1993). Besides, this suggested that a small amount of functional Zas1 or its downstream protein Usp101 is sufficient to bring the zas1-Ts34 mutant back to the normal growth status.

Thus with the above analysis, it is supported that the decreased expression of gene usp101 and thus insufficient functional Usp101 protein is responsible for the temperature sensitive phenotype in the strain with zas1-Ts34 mutation.

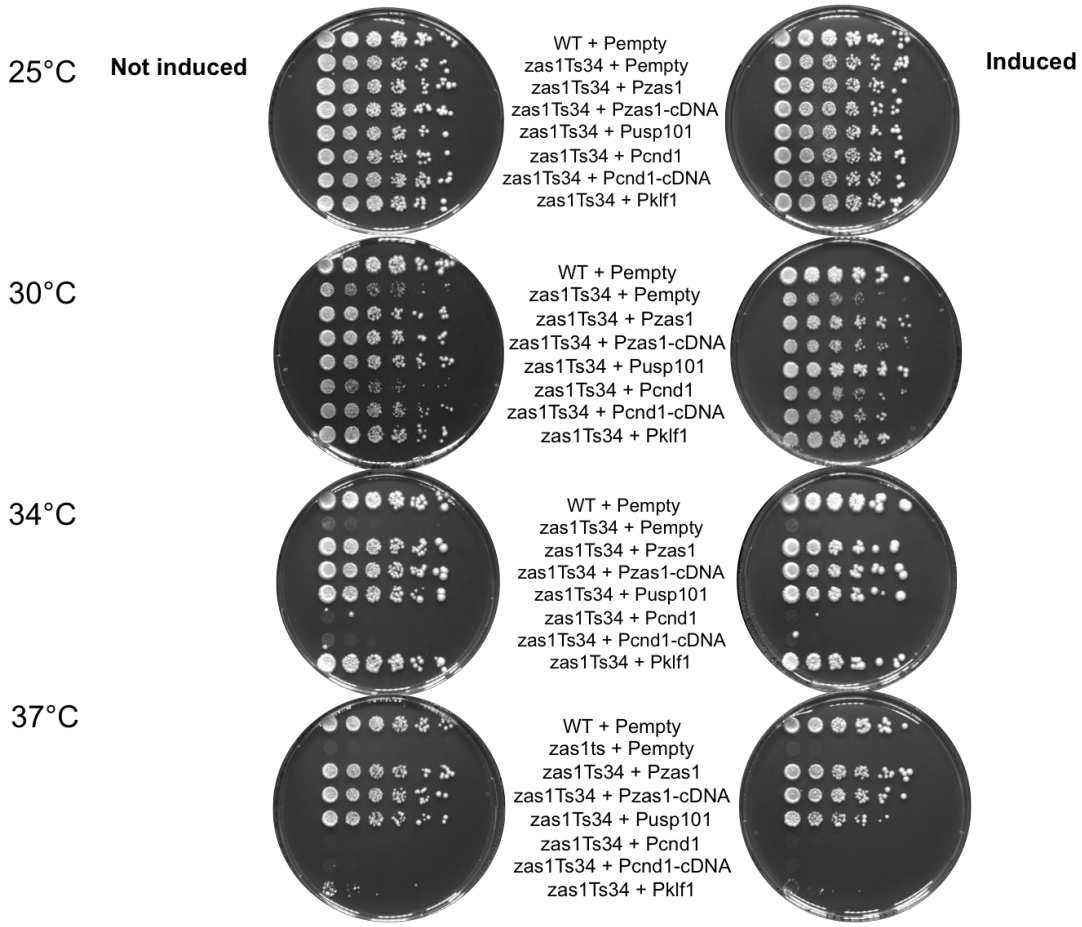

Figure 2.16 Growth test of the PEM2-*zas1Ts34* mutant carrying multicopy plasmids. PEM2-*zas1Ts34* strain carrying either multicopy empty vector or vector containing *zas1, zas1-cDNA*, *usp101*, *cnd1*, *cnd1-cDNA* and *klf1* before and post nmt81 promoter induction were spotted onto selective media (EMM4S without leucine) with and without thiamine for growth test at 25°C, 30°C, 34°C and 37°C. PEM2-WT with empty vector was set as positive control. Plasmids holding *zas1*, *zas1-cDNA* and *usp101* are able to confer growth to the mutant at restrictive temperature. Growth inhibition at restrictive temperature is not alleviated in cells with *cnd1* and *cnd1-cDNA* overexpressed. Strain klf1 overexpressed display temperature lethality at 37°C whilst show normal growth at 34°C. All strains display similar growth phenotype in the promoter induced and noninduced conditions indicating the leakage of the nmt81 promoter.

Chapter 3 Discussion

3.1 Genetic interaction partners provide insights into Zas1 function

The fission yeast Zas1 protein is a C_2H_2 zinc-finger transcription factor that is essential for proper mitotic chromosome condensation (Schiklenk et al. 2018). Using a sequence-specific DNA binding domain, Zas1 regulates the expression of a series of genes, including the gene encoding the Cnd1 as subunit of condensin. However, it had so far not been possible to identify the Zas1 target genes that are responsible for the temperature-sensitive phenotype of *zas1* mutants.

In my study, I undertook two systematic approaches to obtain a deeper understanding of Zas1 function. In the first approach I performed a synthetic genetic array analysis to screen for genetic interaction partners of Zas1. Upon uncoupling the expression of *cnd1* from Zas1 control, the SGA analysis revealed negative genetic interactions between the *zas1-Ts34* mutant and *Δclr4*, *Δcsm1*, *Δmde4* or *Δmug185*. Physical interactions between cnd1/cnd2 and csm1/mde4, which both encode subunits of the microtubule-site clamp monopolin complex, have been reported before (Tada et al. 2011). It is indicated that Pcs1-Mde4 complex function in recruiting condensin onto kinetochores during mitosis. There is also report on negative genetic interaction between *cut3*/*cut14* and *clr4*, which encodes a histone H3 lysine methyltransferase as the heterochromatin marker (Ryan et al. 2012), providing the evidence in the same line since reliable kinetochores attachment and subsequent condensin recruitment depends on the intact structure of centromere heterochromatin.

No genetic interactions between condensin and *mug185* had been previously described. Mug185 encodes the meiotically up-regulated gene protein (Martín-Castellanos et al. 2005). It contains a DnaJ domain (9-74 amino acids) at the N terminus and a zinc finger like motif at the C terminus (270-294 amino acids) (UniProtKB-O14213 (MU185_SCHPO)). DnaJ, also known as Hsp40, is a chaperon protein expressed in various species, ranging from bacteria to mammals. The 'J' in the name DnaJ comes from a conserved N-terminal domain of about 70 amino acid residues. It has been reported that Hsp40 and Hsp70 chaperones cooperate to facilitate protein biogenesis and to renature heat-denatured proteins from deleterious environmental stress (Hennessy et al. 2005; Ohtsuka & Hata 2000; Walsh et al. 2004; Cyr et al. 1994). Hsp40 alone does not have chaperon activity, but functions by stimulating the ATPase activity of Hsp70 protein family by binding to its DnaK domain.

The generated ADP-bound DnaK interacts with polypeptide substrate subsequently and function in preventing proteins from aggregation. The zinc finger region is shown to stabilize the tertiary structure of the DnaJ chaperone and facilitate the interaction between Hsp40 and Hsp70 for protein folding (Linke et al. 2003; Szabo et al. 1996; Banecki et al. 1996).

It is speculated that the genetic interaction between *zas1* and *mug185* might suggest the regulation of Zas1 protein level by Mug185, because DnaJ and DnaK chaperon proteins have been previously found to synergistically bind transcription factors to regulate their abundance. For example, in *Escherichia coli*, the rapid degradation of heat shock transcription factor σ^{32} is tightly regulated by DnaJ and DnaK chaperones (Rodriguez et al. 2008; Suzuki et al. 2012). Another example for the interaction between transcription factors and chaperones is EKLF, which was found to recruit histone chaperones to facilitate the expression of β-globin (Soni et al. 2014). It is hence conceivable that DnaJ and DnaK chaperon complexes might bind Zas1 to regulate its protein levels.

3.2 A multi-copy suppressor screen revealed usp101 as a key target of Zas1

To search for genes that would rescue the temperature-sensitive phenotype of *zas1-Ts34* when overexpressed, I performed a genome-wide multi-copy suppressor screen. In addition to plasmids carrying genomic copies of *zas1* and *klf1*, I discovered that overexpression of *usp101*, which encodes a homolog of the U1 snRNP70, rescues cell growth of the *zas1-Ts34* mutant at the restrictive temperature 34°C.

A re-analysis of available Zas1 ChIP-seq data revealed that Zas1 binds to the promoter region of *usp101*. This suggests that *usp101* is one of the transcriptional targets of Zas1. Indeed, *usp101* mRNA and Usp101 protein expression levels are significantly reduced in the *zas1-Ts34* mutant. Overexpress *usp101* uncoupled from Zas1 control in the mutant has successfully restored the mRNA expression as wild type. Since Usp101 function as essential particle of spliceosome that recognize the 5' splicing site, the speculative hypothesis was therefore raised as that the impairment of Usp101 induces general splicing defect in cell and causes catastrophes in cellular process that eventually lead to the cell death of the *zas1-Ts34* mutant. The transcriptome profile has been mapped and the result supports the hypothesis. The total intron reads and the fraction of unspliced pre-mRNA transcripts are significantly higher in *zas1-Ts34* cells than the one in wild-type cells. Notably, splicing defects in the *zas1-Ts34* mutant can be recovered by overexpressing *usp101*. These observations strongly suggest that *usp101* is one of the key target genes regulated by Zas1 and that the inviability of the *zas1-Ts34* mutant at restrictive temperature is due to reduced expression of *usp101*.

3.3 Implications for human health

Since the open reading frame of an mRNA is easily disrupted due to splicing errors, the precision of every step of splicing – splice site recognition by base pairing of the pre-mRNA with snRNAs, lariat formation, and intron excision – is tightly linked to the fate of all cellular machineries. Furthermore, alternative splicing is employed by the cell as a principal strategy to expand the coding capacity of DNA sequences to generate a vastly extended pool of proteins. The function of the spliceome thereby enables cell differentiation and development. As U snRNPs are constitutively expressed in cells (Vazquez-Arango & O'Reilly 2018), the impairment of any snRNP component will prevent the faithful execution of the spliceosome's pivotal role in pre-mRNA splicing. A significant number of human diseases have been found to be caused directly by mutations that disrupt U snRNP biogenesis. These pathologies all show distinct impairments that affect specific tissues or cells. For example, amyotrophic lateral sclerosis (ALS) is a neurodegenerative disease caused by mutations in the RNA-binding protein FUS/TLS, which result in the mislocalization of the U1 snRNP (Yu et al. 2015; Yamazaki et al. 2012). The autosomal dominant disease retinitis pigmentosa has been ascribed to mutations in the splicing factors HPRPF3 and HPRPF8, which encode proteins facilitating the assembly of the tri-snRNP complex U4/U6-U5 (McKie 2001).

3.4 Future prospects

Although the biogenesis and the assembly of the spliceosome has attracted plenty of research interests in the past (Patel & Bellini 2008; Collins et al. 2009; Vazquez-Arango & O'Reilly 2018; Matera & Wang 2014; Wahl et al. 2009), snRNA transcription control has also been extensively studied (Ohtani 2017; Takahashi et al. 2015; Mroczek & Dziembowski 2013; Cheng et al. 2017), the molecular and genetic mechanisms that regulate the expression of genes that encode the protein components of U snRNPs have not been studied to my knowledge.

My study has documented the role of the transcription factor Zas1 in regulating the expression of the U1 snRNP 70 homolog in fission yeast. Since the splicing machinery is highly conserved from yeast to humans, the understanding of molecular mechanism of U1 snRNP transcriptional control in fission yeast might shed light on the mechanism of the transcriptional regulation of the corresponding machinery in multi-cellular organisms.

The fact that restoring Cnd1 levels by decoupling the *cnd1* gene from the regulative control by Zas1 is not able to restore normal mitotic chromosome condensation (Schiklenk et al. 2018) suggested that the condensation defect in the *zas1-Ts34* mutant might be caused by the combined effect from the misexpression of multiple target genes. Instead, it is conceivable that the condensation defect originates from a general splicing defect that results from a reduction of Usp101 levels. Thus, future experiments will need to test whether restoring Usp101 levels recovers the wild-type chromosome condensation in *zas1-Ts34* mutant cells.

Chapter 4 Methods

4.1 Fission yeast methods

4.1.1 S. pombe strains and growth media

Yeast strains used are listed in Material Table 5.1.
Strains were revived from –80°C stock on the appropriate agar plates 3 days before an experiment and incubated at 25°C. A single colony was picked for inoculation of liquid media. Generally, rich media YE5S (Yeast Extract with 5 Supplements: leucine, histidine, adenine, uracil and lysine; containing antibiotics if required) or EMM2 (Edinburgh Minimal Medium 2) media with specific amino acids supplements were used. Since yeast extract contains thiamine, any strain with integrated or plasmids containing nmt (no information with thiamine) promoter was grown in EMM2-based media. EMM4S is equivalent to EMM2 media supplemented with 4 extra amino acids. Which amino acid is excluded from the media depends on the auxotrophic selection marker in the strain. Note that EMM-based media is not suitable for antibiotic selection. EMM4S without histidine media was used for multi-copy suppressor screening to select for strains maintaining plasmids with the his7^{+} marker. EMM4S without leucine media was used as selection media for plasmids with the *LEU2* marker. Liquid media was prepared according to protocols from 'Fission yeast - A laboratory Manual' (Hagan et al., 2016). Agar plates were prepared by adding 2% Bacto agar.

Cell concentration was measured by spectrometry at a wavelength of 600 nm (OD_{600}). An OD_{600} of 0.5 correlates to 7×10^6 *S. pombe* cells. For each experiment, strains were first inoculated in the corresponding media at 25°C for 24 h as pre-cultures and then diluted to an OD_{600} of 0.1. Experiments were then performed when the cultures reached log phase (OD_{600} of 0.3–0.6, or a cell concentration of 2×10^6 –1×10^7 cells/mL).

4.1.2 S. pombe transformation by LiAc –TE method

Fission yeast cells were cultured in 50 mL YE5S liquid media until the culture reached an OD_{600} of 0.4–0.5. Cells were pelleted at 3,000 rpm for 2 min. The pellet was washed twice with 50 mL of double distilled water (ddH_2O), again pelleting cells at 3,000 rpm for 2 min. The pellet was then re-suspended in 50 mL of LiAc-TE and pelleted again at 3,000 rpm for 2 min. The pellet was re-suspended in 400 µL of LiAc-TE. To 100 µL of cell suspension, 10 µL of salmon sperm DNA (heated to 95 °C for 5 min and cooled down to room temperature before use) was added and gently mixed. The mixture was incubated

at room temperature for 10 min. Addition of salmon sperm DNA facilitates the entry of target DNA by binding to the cell wall of *S. pombe*, saturating binding sites and preventing degradation of the target DNA by *S. pombe* nucleases.

Up to 10 µL of target DNA was added to the cell suspension and the mixture was incubated at room temperature for 10 min. 280 µL of 40% PEG500 in LiAc-TE was added and mixed thoroughly and gently. This suspension was incubated at room temperature for 1 h. 43 µL (10%) of DMSO were added gently and mixed thoroughly. The mixture was moved to a heating block at 42°C for 7 min.

The cell suspension was then pelleted immediately at 3,000 rpm for 2 min at room temperature. The pellet was washed three times with 1 mL of ddH_2O and re-suspended in 200 µL of ddH_2O. If plasmids were transformed, the cells were plated directly onto the desired selection media. If PCR-based homologous recombination was required, the pellet was re-suspended in 5 mL of YES and incubated at 25°C overnight for recovery before plating onto selection media.

4.1.3 Genetic crosses and tetrad dissection

Mating by crossing *S. pombe* strains with strains of the opposite mating type (h^+ or h^-) is frequently used to obtain strains with a preferred genotype. Strains stored in glycerol at –80°C were revived on a YE5S plate and incubated at 25°C for 3 days. Freshly grown h^- and h^+ cells were picked off the YE5S agar plate with a toothpick tip and transferred into 20 µL of ddH_2O. Cells were mixed thoroughly by gentle pipetting and plated onto SPAS agar plates to cover an area of about 1 cm^2 (SPAS media was used because conjugation and sporulation only takes place under conditions of nitrogen starvation). The plate was incubated at 25°C for two days and the extent of sporulation was monitored in a transmission light microscope. A small fraction of sporulated cells was transferred into 200 µL ddH_2O. A drop of cell suspension was placed into the center of a fresh YES agar plate and this plate was incubated at 25°C for 24 h to allow for the digestion of the ascus wall. Using a Singer MSM 400 Dissection Microscope, the four spores of an ascus were placed about 3 mm apart in a line on the YES plate. The plates were incubated at 25°C for about 4 days until colonies formed.

4.1.4 Genomic DNA extraction from S. pombe for general use

This protocol was used to obtain genomic DNA for general use, such as validation of genetic modifications by homologous recombination or as template for PCR. Genomic DNA was extracted using the Quick-DNA™ Fungal/Bacterial Miniprep kit (D6005, Zymo Research) following the manufacturer's protocol.

4.1.5 Plasmid isolation from S. pombe

Plasmids were isolated from *S. pombe* by the Zymoprep™ Yeast Plasmid Miniprep I kit (Cat. No. D2001) following the manufacturer's instructions. The key component provided by the kit is the enzyme mixture, which contains multiple enzymes to lyse yeast cell wall. 1 mL of yeast culture with OD_{600} above 1.0 was pelleted. 150 µL of digestion buffer (Solution 1) and 2 µL of Zymolyase mixture was added to the tube and incubated at 37°C for 60 min. 150 µL of lysis buffer (Solution 2) and neutralizing buffer (Solution 3) were added subsequently after the incubation. The suspension was pelleted at 13,000 rpm for 2 min. The supernatant was collected and transferred to a new 1.5 mL Eppendorf tube. 400 µL of isopropanol was added to the supernatant to precipitate the DNA. DNA was pelleted by centrifugation at 14,000 rpm for 8 min. The supernatant was discarded and the pellet was dissolved in 35 µL of TE buffer.

4.1.6 Synchronization of fission yeast by hydroxyurea

Depending on the strain background and specific experimental conditions, various ways of synchronization can be chosen. In this work, due to the temperature sensitivity of the strains with a *zas1* ts mutation, *S. pombe* cells were synchronized via the hydroxyurea method (Tormos-Pérez et al., 2016). Hydroxyurea (HU) is an inhibitor of ribonucleotide reductase and inhibits DNA replication. HU does not prevent cell division, thus *S. pombe* arrested by HU are synchronized at early S phase with a single copy of their genomic DNA (Tormos-Pérez et al., 2016).

Yeast cell cultures were grown at 25°C until an OD_{600} of 0.3–0.5. Two samples were taken from each time point as technical replicates. Before addition of HU, 2 mL of cultures were taken as 'asynchronous cells' sample. The amount needed from a 1 M HU stock solution was calculated and added o the yeast culture to reach a final concentration of 12 mM. The culture containing HU was incubated at 25°C for an additional 4 h. A 2mL sample was taken at the 4 h time point ('early S phase' sample).

To release cells into the cell cycle, HU needs to be removed thoroughly from the culture. This can be done either by centrifugation of the cells or by cell filtration, followed by washing the cells with medium at the preferred temperature. As the latter method consumes less time and exposes cells to less stress, cell filtration was chosen. Half of the cell culture was filtrated and washed with 80 mL of YE5S media at 25°C for 4 times and cells were then re-suspended in 50 mL of YE5S media at 25°C. The other half of the culture was filtrated and washed with 80 mL of YE5S pre-warmed to 34°C for 4 times. Cells were then re-suspended in 50 mL of YE5S at 34°C. Cells were re-suspended by placing the filter paper into the medium and shaking. Both cultures were then adjusted to OD_{600} of 0.2.

The cultures were incubated at the appropriate temperature and 2 mL samples were collected every 30 min for 2 h. The cultures were incubated at the respective temperatures overnight to obtain the final sample in the next morning. To monitor cell cycle progress by flow cytometry, each sample was pelleted and fixed using cold 70% ethanol (prechilled at –20°C) immediately after the sample collection.

4.1.7 DNA content measurement of S. pombe by flow cytometry

4.1.7.1 Sample fixation for flow cytometry analysis

Samples in 2 mL Eppendorf tubes taken at the appropriate time points were pelleted immediately at 3,000 rpm for 2 min. Tube were placed onto a vortex and cells were fixed by adding 1 mL of cold 70% ethanol (prechilled at –20°C) while keeping the tube in vortex. This avoids formation of cell aggregates. Fixed samples were stored at 4°C for at least 15 min before use. According to Sabatinos and Forsburg (2009), they can be stored at 4°C for 1 year or more.

4.1.7.2. Re-hydration and staining of fixed fission yeast cells for FACS

To ensure that the FACS data produces quantitative results, each sample should have same amount of cells. Fixed samples were vortexed and cell concentration was measured using a spectrophotometer. 1×10^7 cells were taken out of each sample and pelleted at 3,000 rpm for 2 min. The pellet was washed twice with 1 mL of 20 mM EDTA pH 8.0 (Boye et al., 2016). RNA in the samples was digested with RNase A by re-suspending the pellet in 300 µL of 20 mM EDTA containing 100 µg/mL RNase A and incubating at 36°C for 3 h to overnight.

Samples were then mixed 1:1 with Sytox Green-EDTA solution (4 µM Sytox Green in 20 mM EDTA). The stained samples were stored at 4°C in the dark for at least 15 min before sonication. Sytox Green (SYTOX® Green-S7020, ThermoFisher) is a nucleic acid stain that is excited at 488 nm. Sonication was conducted right before flow cytometry to prevent cell aggregation. Samples were sonicated in a G. Heinemann sonifier W-250 D with a 3 mm micro tip at 4°C. The entire sample was sonicated at an amplitude of 25 % for 5 s with 1 s bursts and 0.5 s off in turn. Samples were kept on ice after sonication and protected from light before analysis. 5 mL BD Falcon polystyrene tubes were provided by the EMBL Flow Cytometry Facility. Stained cells were analyzed using the BD LSRFortessa™ cell analyzer with a low flow rate. DNA content was measured based on both DNA area (DNA-A) with pulse width (DNA-W) and forward (FSC) with side light scattering (SSC) of the Sytox green signal excited at 488 nm.

4.1.8 Total RNA extraction from fission yeast

Total RNA was extracted by the hot phenol method as described by Bähler and Wise (2017) with modifications. In this protocol, it is important not to process more than 6 samples in parallel, since delays can compromise the quality of the RNA. Residual DEPC not destroyed by autoclaving can react with adenines in the RNA, thus RNase-free ddH_2O provided by the EMBL media kitchen was used in the procedure rather than DEPC water.

Cells were cultured in the appropriate media and 25 mL of culture were harvested at an OD_{600} of 0.3 for each sample. Cells were collected by centrifugation at 2,000 rpm for 2 min and the supernatant was discarded. Centrifugation speed and time were limited to avoid activation of the stress response pathway (Lawrence et al., 2007). The cell pellet was collected in 2 mL Eppendorf tube and snap frozen immediately in liquid nitrogen and stored at –80°C for later RNA extraction.

To begin the extraction step, samples were thawed on ice for 5 min and cells were resuspended in 1 mL of pre-chilled DEPC water. Cells were collected by centrifugation at 5,000 rpm for 10 s and supernatant was removed. Cells were resuspended in 750 µL of TES buffer with tubes transferred into the hood and 750 µL of acidic phenol-chloroform (pre-chilled to 4°C) added immediately.

Before continuing with the next samples, the tube was vortexed and incubated at 65°C in the hood. Then the next sample was processed in the same way. All samples were incubated at 65°C for 1 h and vortexed for 10 s every 10 min.

Phase lock tubes with MaXtract gel (Cat No. 129056, Qiagen) were used to separate the aqueous from the organic phase. All phase lock tubes were pre-spun at 13,000 rpm to pellet the MaXtract gel at the bottom of the tube. 700 µL of acidic phenol-chlorofom was added to each phase lock tube. 700 µL of the top aqueous layer from the tube with cell mixture obtained after heat treatment was taken to the phase lock tube with acidic phenol-chloroform. The tube was gently mixed by inverting and pellet for 5 min at 20,000×g at 4°C. Prepare another batch of phase lock tubes by pre-spinning. 700 µL of chloroform:isoamyl alcohol (24:1) were added to each phase lock tube. 700 µL of the top water phase from the first phase lock tube after centrifugation was added to the second phase-lock tube. Mix gently and thoroughly by inverting.

Pellet the tube for 5 min at 14,000 rpm at 4°C. Standard 2 mL Eppendorf tubes containing 1.5 mL 100% EtOH (pre-chilled to –20 °C) and 50 µL of 3 M NaOAc pH 5.2 were prepared. 500 µL of the top aqueous phase from the second phase lock tube after centrifugation were carefully transferred to the prepared 2 mL Eppendorf tubes. The tubes were vortexed for 10 s and incubated at –80 °C for at least 30 min or at –20°C overnight for precipitation. The tubes were centrifuged at 14,000 rpm for 10 min at 4°C, the supernatant was discarded and the pellet was washed by addition of 500 µL of 70% EtOH (prepared with double distilled water (ddH_2O) and pre-chilled to 4°C). Tubes were mixed by flicking with a finger and centrifuged again in the same orientation to avoid dislodging the pellet. The supernatant was aspirated and the rest of liquid was removed after further short spinning for 5 seconds. The pellet was air dried at room temperature for 15 min.

To dissolve RNA, 100 µL of ddH_2O was added and tubes were incubated at room temperature for 10 min. The concentration of total RNA was measured using nanoscale spectrophotometer (NanoDrop). For RNA-seq experiments, 100 µg of total RNA from each sample was further purified using the RNeasy mini RNA purification kit (Qiagen) following the manufacturer's protocol. In the final step, RNA was eluted twice with 30 µL of RNase-free water and kept on ice. The quality of the RNA preparation was assessed by running 2 µL of purified RNA on a 1% agarose gel on a Bioanalyzer, which generated a 'virtual gel' from the electropherogram and measured the amount of RNA. The volume of the remaining RNA was measure and stored as backup at –80°C after gently mixing with 1/10-volume of 3 M NaOAc (pH 5.2) and 3 volumes of 100% ethanol.

4.1.9 Multi-copy suppressor screening

Strain FWP60 (*his7-366*) was crossed with a PEM2-*zas1-Ts34* strain to obtain the host strain FWP60-PEM2-*zas1-ts34* (irrelevant auxotrophy markers in the strain are not listed). The genomic DNA library was developed by the Hoffman lab (Wang et al., 2005) and provided as a gift. This library is in the vector pEA500, which contains as *his7*$^{+}$ selection marker (Apolinario et al., 1993). 70% of the library plasmids contain a DNA insert and the average size of the inserts is 3.9 kb.

The genomic DNA library was first amplified in DH5-alpha *E. coli* cells. About 6×10^{4} clones were obtained during the amplification step. The sum of insert DNA in these clones covers about 20 times the genomic size of *S. pombe*. Plasmids were extracted from these clones using the HiSpeed Plasmid Maxi Kit (Qiagen, 12662). To conduct the suppressor screening, the host strain FWP60-PEM2-*zas1-Ts34* (*his7-366*) was transformed with the amplified genomic DNA library following the LiAc/TE protocol and cells were plated onto EMM4S (without histidine) agar plates and incubated at 25°C for 6 days.

About 42,000 *his*$^{+}$ colonies were replica plated onto a new batch of EMM4S (without histidine) plates and incubated at the *zas1-Ts34* restrictive temperature 34°C for 6 days. This step selected 48 clones, which remained viable at the restrictive temperature. Plasmids from all these clones were isolated using the yeast plasmid extraction kit (Cat. No. D2001, Zymoprep™ Yeast Plasmid Miniprep I) and transferred into *E. coli*. Then all plasmids were transformed back into the host strain to validate suppression of the ts phenotype by plating onto selective media and incubation at 34°C for 6 days. Only 9 clones were recovered from this validation test. Plasmids were retrieved again from these clones and amplified in *E. coli* and sequenced using vector-specific primers.

4.1.10 Synthetic genetic analysis (SGA)

Both query and control query strain were inoculated into 20 mL YE5S liquid medium at 25°C and incubated overnight. The query strain cultures were replica plated from the liquid culture onto YES5S agar plates when OD_{600} reached 0.8. All high-throughput screening procedures were performed with the Rotor HDA platform (Singer Instruments) on PlusPlates (Singer Instruments, PLU-003). In this first replica step, the 'Bath' program was selected as the query format and the 384 long pin program was selected to replica cells from the liquid culture to agar plates.

The Bioneer V5 *S. pombe* haploid deletion library is an *S. pombe* strain library with 3,420 haploid deletion mutants, covering 95.3% of the non-essential genes. The deletion library was thawed from a –80°C stock and replica plated onto YE5S agar media in the 384 format and grown for 3 days at 25°C. Since the original Bioneer V5 library is arrayed in 36 plates of the 96 format, it was first replica plated onto 9 plates in the 384 format. In order to ensure the identity of the strains, both query and library strains were replicated to YE5S agar media plus the respective antibiotic and grown for another 3 days at 25°C (the query strain was replicated ontoYE5S with clonNat (100 mg/L), the library strains were replicated onto YE5S with geneticin (100 mg/L) agar plates).

For the mating step, the corresponding 'Mating' program was selected for the Rotor HDA platform. Query and library strains were subsequently replica plated onto the same SPAS media plate and mixed well with additional tip of ddH_2O. SPAS plates were incubated at 25°C for 3 days to allow cells to sporulate. Cells on SPAS plates were then transferred to new YE5S agar plates and incubated at 25°C for 2 days. This step ensured that cells germinated before further selection. Two rounds of selection were then performed to isolate double mutants, three rounds of selection were applied to isolate triple mutants.

For the first selection step, cells were incubated at 25°C for 2 days on YE5S plus cycloheximide (100 mg/L, abcam ab120093) and geneticin (G-418 sulphate, 100 mg/L, Life Technologies CAS No. 108321-42-2). Cycloheximide selects for cells with mating type h^+ and to remove remaining diploids and unmated parental cells. According to Roguev et al., (2007), addition of geneticin at this step provides a better signal-to-noise ratio when compared to addition of cycloheximide alone.

For the second selection step, cells were replica plated from YE5S+G+C onto YE5S media with clonNat (nourseothricin, 100 mg/L, Jena Bioscience CAS No. 96736-11-7), geneticin (100 mg/L) and cycloheximide (100 mg/L) in triplicate and one plate was incubated at 25°C for 3 days. Since haploid cells with the *zas1-ts34* mutation are not viable at a restrictive temperature 34°C and above, most haploid double mutants obtained should also be lethal at this temperature unless the second deletion acts as a genetic suppressor. Thus, the two other replica plates were incubated at 34°C and 37°C respectively to test the efficiency of the selection. After three days, images of the plates were taken using a spImager S&P Robotics with a Canon Rebel T3i camera. This instrument has specifically been developed for PlusPlates imaging to minimize reflection spots, which interfere with further image analysis.

The SGATools software package (http://sgatools.ccbr.utoronto.ca/) was applied to process images and to extract colony size in pixels following the instruction on the SGATools platform. The information of colony sizes was then uploaded into the SGA analysis tool for data analysis. The SGA analysis tool was developed by StJohn Townsend (Bähler lab, scripts unpublished).

4.2 Nuclei acid and protein methods

4.2.1 PCR mutagenesis

Site-directed mutagenesis was used to introduce single nucleotide mutations. Overlapping Primers with the desired mutation were designed in reverse orientation. After amplification by PCR, the reaction was treated with DpnI at 37°C for 1 h to digest the template plasmid. The double-nicked plasmids with the mutation were directly transformed into chemical competent DH5-alpha *E. coli* cells.

For in-fusion mutagenesis, primers containing the desired the mutation were designed in a back-to-back orientation. In-fusion mutagenesis was performed following the manufacturer's protocol (In-Fusion® HD Cloning Plus, Clontech).

4.2.2 Large-scale amplification of plasmids

First, a small scale amplification was performed to assess the number of colonies that can be obtained from a standard transformation and from this, the amount of clones that cover 20 times the genome size of *S. pombe* was calculated. 2 µL of the genomic DNA library plasmids (189 ng/uL) were transformed into 100 µL of competent DH5-alpha cells by electroporation. DH5-alpha cells were then diluted with 10 mL of LB media with 100 mg/L ampicillin and incubated at 37 °C for 30 min. After recovery, all transformed DH5-alpha cells were plated onto twenty 15 cm × 15 cm LB-ampicillin agar plates (500 µL of the transformed DH5-alpha cell culture per plate). Plates were incubated at 37°C for 18 h and the amount of colonies on one plate was counted to assess the coverage. All colonies were collected with a sterile glass rod and purified using a HiSpeed Plasmid Maxi Kit (Qiagen 12662) according to the manufacturer's instructions.

4.2.3 Protein extraction and western blotting

S. pombe cultures were grown to an OD_{600} of 0.5. The same amount of cells with OD 5 was collected from each culture as sample. Each sample was washed twice with 1 mL of ddH_2O. Protein was extracted as described in Matsuo et al. (2006). The cell pellet was re-suspended in 0.3 mL of ddH_2O following with 0.3 mL of 0.6 M NaOH addition. The mix was incubated at room temperature for 5 min. Cells were pelleted by centrifugation at 3,000 rpm for 2 min and the supernatant was discarded.

The cell pellet was re-suspended in 70 µL of Matsuo buffer (Matsuo et al., 2006) and the suspension was heated at 95°C for 5 min. Cell debris was pelleted at 14,000 rpm for 5 min at room temperature and 15 µL of the supernatant from each sample was loaded onto a NuPAGE™ 4-12% Bis-Tris protein Gel (ThermoFisher NP0321). Gels were run in MOPS buffer at 175 V with maximum currency for 65 min.

A PVDF membrane (Bio-Rad 162-0177) of the same size as the SDS-PAGE gel was activated by incubation in methanol for 2 min and rinsed with ddH_2O. The SDS-PAGE gel was equilibrated in transfer buffer together with the prepared PVDF membrane and 4 pieces of Whatman paper for 15 min. The blotting stack was assembled in a Trans-Blot Turbo transfer system (Bio-Rad 1704155), using two pieces of soaked Whatman paper as the bottom layer, followed by the PVDF membrane, the SDS-PAGE gel and another two pieces of Whatman paper as the top layer. Samples were blotted at a voltage of 25 V for 25 min.

After transfer, the membrane was first blocked with 25 mL of blocking buffer for 30 min with shaking. 1 µL of the primary antibody detecting the tag of interest was diluted into 10 mL of blocking buffer in a 50 mL Faclon tube and the membrane was added to the tube. The tube was incubated on a roll shaker at room temperature for 1 h or at 4 °C overnight. The primary antibody solution was stored at −20°C and re-used for up to 4 times. The membrane was then washed three times by incubating in the washing buffer for 10 min each. The membrane was then transferred into 10 mL of blocking buffer with 1 µL of secondary antibody (conjugated horse radish peroxidase targeting the corresponding first antibody) in a 50 mL Falcon tube and incubated at 4°C for 1 h. The membrane was washed three times as before and then placed onto a plastic foil. 100 uL of each Enhanced chemiluminescence (ECL) reaction solution (Advansta K-12045-D20) was mixed and used to cover both sides of the membrane. Chemiluminescence was detected using the ChemiDoc Imaging system (Bio-Rad). After the exposure step, the membrane was washed three times using washing buffer. The western blot was repeated using antibody antiTAT1 to detect the tubulin as the loading control.

4.3 RNA-seq analysis

RNA-seq data was analyzed by Lin Gen (Bioinformatics Scientist, Steinmetz lab, Genome Biology Unit, EMBL)

The general procedure of RNAseq analysis was performed as following. *Schizosaccharomyces pombe genome* fasta and gff file were downloaded from Pombase (www.pombase.org). Reads were aligned to the *Schizosaccharomyces pombe* genome using tophat2 (v2.1.1) (Kim 2013), with splice junctions provided using the —juncs option and a minimum intron size of 5 and maximum intron size of 5,000. After alignment, reads falling inside exons and introns were counted using count. Only uniquely aligned reads were used for genomic alignments. Differential gene expression (using only exon counts) or intron expression aggregated by gene were assessed using DESeq2, using total library size for size factor normalization.

Chapter 5 Materials

5.1 Fission yeast methods

10 X TE

Tris-HCl	100 mM, pH 7.5
EDTA	10 mM

1 M LiAc stock

1 M LiAc dissolved in ddH2O. Sterilized by autoclaving.

0.1 × LiAc-TE buffer (fission yeast transformation)

LiAc	100 mM
Tris-HCl	10 mM, pH 7.5
EDTA	1 mM

5.2 Fission yeast media

YE5S (Yeast Extract with five supplements)

Yeast Extract	5 g/L (Bacto ™, 212750)
glucose	30 g/L
histidine	225 mg/L
adenine	225 mg/L
uracil	225 mg/L
lysine	225 mg/L
leucine	225 mg/L

EMM5S (Edinburgh minimal medium with five supplements)

glucose	20 g/L
NH_4Cl	5 g/L
Potassium hydrogen phthallate	3 g/L
Na_2HPO_4	2.2 g/L
1000 × Vitamins	1 mL/L
50 × salts	20 mL/L
10,000 × minerals	0.1 mL/L
histidine	225 mg/L
adenine	225 mg/L
lysine	225 mg/L
leucine	225 mg/L
uracil	225 mg/L

EMM4S (no histidine): exclude the histidine from the EMM5S recipe.
EMM4S (no leucine): exclude the histidine from the EMM5S recipe.

1000 × Vitamin stock

inositol	10 g/L
nicotinic acid	10 g/L
pantothenic acid	1 g/L
biotin	10 mg/L

50 × Salt stock

$MgCl_2 \cdot 6H_2O$	52.5 g/L
KCl	50 g/L
Na_2SO_4	2 g/L
$CaCl_2 \cdot 2H_2O$	0.735 g/L

10,000 × Mineral stock

boric acid	5 g/L
citric acid	10 g/L
$ZnSO_4 \cdot 7H_2O$	4 g/L
$MnSO_4$	4 g/L
$FeCl_2 \cdot 6H_2O$	2 g/L
KI	1 g/L
$CuSO_4 \cdot 5H_2O$	0.4 g/L
molybdic acid	0.4 g/L

SPAS (nitrogen deprived mating media)

glucose	10 g/L
1000 × vitamins	1 mL
KH_2PO_4	1 g/L
histidine	45 mg/L
uracil	45 mg/L
lysine	45 mg/L
leucine	45 mg/L
adenine	45 mg/L

5.3 Nuclei acid and protein methods

TES

Tris-HCl	50 mM, pH 8.0
SDS	1 % (w/v)
EDTA	10 mM

Modified SDS-sample buffer (Matsuo et al. 2006)

2-mercaptoethanol with final concentration of 4 % was added freshly before use.

SDS	4 % (w/v)
Bromphenol blue	0.01 % (w/v)
Tris-HCl	60 mM
glycerol	5 % (v/v)

20 × MOPS stock (MOPS: running buffer for Bis-Tris-SDS-PAGE gel)

3-Morpholinopropane-1-sulfonic acid (MOPS)	0.4 M
NaOAc	0.1 M
EDTA	0.02 M
NaOH	Adjust the pH to 7.0

50 × TAE (running buffer for agarose gel electrophoresis)

Tris-HCl	2 M
glacial acetic acid	5.75 % (v/v)
EDTA	50 mM (pH 8.0)

5.4 Strains and primers used in this thesis

Table 5.4.1 *S. pombe* strains used in this thesis

Strain Name	Genotype	Source
972	*h⁻*	Lab stock
2457	*h⁺/h⁻; diploid, ade6-M210/ade6-M216*	Brunner lab
PEM2	*h⁻; ade6-M210, leu1-32; ura4-D18, mat1_m-cyhS, smt0; rpl42::cyhR (sP56Q)*	(Roguev et al. 2007)
PEM2-zas1Ts34	*h⁻; zas1::zas1-Ts34-natMX6, ade6-M210, leu1-32; ura4-D18, mat1_m-cyhS, smt0; rpl42::cyhR (sP56Q)*	this work
PEM2-zas1Ts34 P_{cnd3}-cnd1	*h⁻; zas1::zas1-Ts34-natMX6, P_{cnd1}-cnd1::hphMX6-P_{cnd3}-cnd1, ade6-M210, leu1-32; ura4-D18, mat1_m-cyhS, smt0; rpl42::cyhR (sP56Q)*	this work
PEM2-ade6Δ	*h⁻; ade6::ade6Δ -natMX6, leu1-32; ura4-D18, mat1_m-cyhS, smt0; rpl42::cyhR (sP56Q)*	this work
PEM2-ade6Δ P_{cnd3}-cnd1	*h⁻; ade6::ade6Δ -natMX6, P_{cnd1}-cnd1::hphMX6-P_{cnd3}-cnd1, leu1-32; ura4-D18, mat1_m-cyhS, smt0; rpl42::cyhR (sP56Q)*	this work
975- ade6Δ	*h⁺; ade6::ade6Δ -kanMX6*	this work
FWP60	*h⁺; leu1-32, his7-366*	(Apolinario et al. 1993)
FWP60-PEM2	*h⁺; his7-366, ade6-M210, leu1-32, mat1_m-cyhS, smt0; rpl42::cyhR (sP56Q)*	this work
FWP60-PEM2-zas1Ts34	*h⁺; zas1::zas1-Ts34-natMX6, his7-366, ade6-M210, leu1-32, mat1_m-cyhS, smt0; rpl42::cyhR (sP56Q)*	this work
PEM2-zas1Ts34+ p-empty	*h⁺; zas1::zas1-Ts34-natMX6, his7-366, ade6-M210, leu1-32, mat1_m-cyhS, smt0; rpl42::cyhR (sP56Q); pREPNTAP empty vector (LEU2)*	this work
PEM2-zas1Ts34+ p-zas1	*h⁺; zas1::zas1-Ts34-natMX6, his7-366, ade6-M210, leu1-32, mat1_m-cyhS, smt0; rpl42::cyhR (sP56Q); pREPNTAP-zas1 (LEU2, zas1⁺)*	this work
PEM2-zas1Ts34+ p-zas1-cDNA	*h⁺; zas1::zas1-Ts34-natMX6, his7-366, ade6-M210, leu1-32, mat1_m-cyhS, smt0; rpl42::cyhR (sP56Q); pREPNTAP-zas1-cDNA(LEU2, zas1⁺)*	this work
PEM2-zas1Ts34+ p-usp101	*h⁺; zas1::zas1-Ts34-natMX6, his7-366, ade6-M210, leu1-32, mat1_m-cyhS, smt0; rpl42::cyhR (sP56Q); pREPNTAP-usp101(LEU2, usp101⁺)*	this work
PEM2-zas1Ts34+ p-cnd1	*h⁺; zas1::zas1-Ts34-natMX6, his7-366, ade6-M210, leu1-32, mat1_m-cyhS, smt0; rpl42::cyhR (sP56Q); pREPNTAP-cnd1(LEU2, cnd1⁺)*	this work
PEM2-zas1Ts34+ p-cnd1-cDNA	*h⁺; zas1::zas1-Ts34-natMX6, his7-366, ade6-M210, leu1-32, mat1_m-cyhS, smt0; rpl42::cyhR (sP56Q); pREPNTAP-cnd1(LEU2, cnd1⁺)*	this work
PEM2-zas1Ts34+ p-klf1	*h⁺; zas1::zas1-Ts34-natMX6, his7-366, ade6-M210, leu1-32, mat1_m-cyhS, smt0; rpl42::cyhR (sP56Q); pREPNTAP-klf11(LEU2, klf1⁺)*	this work

Table 5.4.2. Primers used in this study

Primer Name	Sequence 5' to 3'
zas1-Ts34 truncation fw 1	CTTTTGCCAAAGCTGTCACCGATCCGGTAGATGGTTCTGTAACCTCAAAAACTGTTGCACC GTTACGATATGTAAAAATACGTACGCTGCAGGTCGAC
zas1-Ts34 truncation fw 2	CATCCTTTCGTTAAGGAGTGCAGATCACTTTATAATTTAGCATGCATCTACTCAAAGACCC GTCTAACCTATTTACAGGCTTTTGCCAAAGCTGTCACCG
zas1-Ts34 truncation rev 1	ATTTAATAAGATGTCATAAGCTGCTATAACTTCGAGTAGATTTATAATCGGCATTAAATA AAATTTACCTCAGTTTATAATATCGATGAATTCGAGCTCG
zas1-Ts34 truncation rev 2	AGTAAGAAAATTAAGCAAAAAATACATAAAAAGGTTACCTGAGTTTAATAATTAATTTTT TATTCCAGAAATATTTAATAAGATGTCATAAGCTGCTAT
zas1-Ts34 3' end seq	GATGGCTGGTGCTCTCTTG
REPNTAP plasmid seq 1	GACAGAATAAGTCATCAGCGG
REPNTAP plasmid seq 2	CAATTTTGGGAATAGCGCAAG
REPNTAP plasmid seq 3	ATATTACGATTTTGTTTTTCG
REPNTAP plasmid seq 4	CGATTGCTAACCACCTATTGG
REPNTAP plasmid seq 5	AGCGGCCATTCTTGTGATTC
REPNTAP plasmid seq 6	GATTTTCTTAACTTCTTCGGCG
REPNTAP plasmid seq 7	CTTTACGAGGCAAAAATGTCGG
T3 to seq pEA500 plasmid library	GCAATTAACCCTCACTAAAGG
T3 to seq pEA500 plasmid library	TAATACGACTCACTATAGGG
ade6 deletion by natMX6 fw 1	CGTTTTTTCAACATTTACCATCTCATTAAGCTGAGCTGCCAAGGTATATACATACTTCATC GAAT CGTACGCTGCAGGTCGAC
ade6 deletion by natMX6 fw 2	GAATTAATACGATGCAAAACTCAAATAATAAACTGCGCACTAACTCACTACAATAAACAA CTTTGAAAAAAAGATT CGTTTTTTCAACATTTACCATC
ade6 deletion by natMX6 rev 1	TTAATTGCGTCGCAGCACATTATTCGGGGGGTTTTTATTTTTAATTTTTAATCACTTTTTA GAATACATTTTACAATCT ATCGATGAATTCGAGCTCG
ade6 deletion by natMX6 rev 2	TGCTTTATAGCATATTATATTGGGTTCTTTAATTTTCTTTCAACTGCTTCACAGCACATTA TTCAGGATTCTTATTTTTT TTAATTGCGTCGCAGCAC
natMX6 cassette seq	GCACTGGATGGGTCCTTC
ade deletion seq fw	CTGCACTTGGTTCGACGAC
ade deletion seq rev	CAATCAGCGCCAATGTTATC
pREPNTAP-zas1 fw	CTTGATTATGGCGCGCCCCATATGTCGACGATGTCAAATGAGGAATCTTTTAC
pREPNTAP-zas1 rev	GCCGCCCCGGGGATCCGTCGACATATGG TTAATCATTTCCCTTGGAT
pREPNTAP-zas1 seq 1	ATGTCAAATGAGGAATCTTTTAC
pREPNTAP-zas1 seq 2	TTAATCATTTCCCTTGGAT
pREPNTAP-zas1 seq 3	CAAGGTGAACTAAAAACTGC
pREPNTAP-zas1 seq 4	CTGTCGTACAATTTTATTCAG
pREPNTAP-zas1 seq 5	GATCTTCCATCGCCTCCTC
pREPNTAP-zas1 seq 6	GGTTTGTTATTCACTGATG
pREPNTAP-zas1 seq 7	GCTTCTTCTTCATGGGTTG
pREPNTAP-zas1 seq 8	GAAGAAGTCACTAATTTGC
Pnmt promoter seq 1	AGACTTTGAATGAAGCCG
Pnmt promoter seq 2	GATTCCATTTTTAATAAGGC
Pnmt promoter seq 3	ATTTATATTTTCCGCAGGATC
Rpl42 gene cyclohexemid sensitive fw	ATGGTGAACATTCCCAAGACC
Rpl42 gene cyclohexemid sensitive rev	CAAATTCGTCTAAATCCAATCCACTCG
rpl42 cyclohexemid resistant allele fw	CCGTGCACCGTGTTACTCAGTAT
rpl42 cyclohexemid resistant allele rev	TCCACCCAATTCGAAGTGCTTGC
replace cnd1 promoter to hphMX-Pcnd3 fw 1	GAACAATAGCTTTTACGTGGCACGCTCAATAAAAGTTAATTAAAATATTATTTTTTAATG TAAACAAATGAGTTAATAA CGTACGCTGCAGGTCGAC
replace cnd1 promoter to hphMX-Pcnd3 fw 2	AGAATTTACAACTAACGTTATTCAAAAAATATATTAAATTCTTTTCAAAACATTTAATTA GAAGTACTAAAAA GAACAATAGCTTTTACGTGGCAC
Pcnd3 replacement seq fw	GCACAAATGCTTACCTCGTC
Pcnd3 replacement seq rev	AGGAAGAGAGGTCAGCAAAGTG
usp101 promoter fw	ACATATTTGCTTCCCTTTTATGTCA

usp101 promoter rev	GTGTAGGGTATATCCCAGTAAAGC
usp101 seq 1	GCATTGTTTGCTCCACGTCC
usp101 seq 2	TGATCGTGAGACTGCGCATA
usp101 seq 3	GCCTCCTATGGATGTGCCTC
usp101 seq 4	TCCAAGCTTTCAGTCGGGTG
pREPNTAP-cnd1 fw	CTTGATTATGGCGCGCCCCAAATGTCGTTGGATCTTCTTTC
pREPNTAP-cnd1 rev	TTTTAGAGCTCGGTACCCGCGCTAGAATGTGCAAATTACTTAGC
pREPNTAP-klf1 fw	CTTGATTATGGCGCGCCCCACATGACCAAGGCGAAAAAAAG
pREPNTAP-klf1 rev	TTTTAGAGCTCGGTACCCGCTTTCTAATGATATTCTGAACATATTAATCAC
pREPNTAP-usp101 fw	CTTGATTATGGCGCGCCCCAAATGGCTGAAAAATTACCG
pREPNTAP-usp101 rev	TTTTAGAGCTCGGTACCCGCAAATTAATAATGATGCATTCAGAG
pREPNTAP-zas1 fw	CTTGATTATGGCGCGCCCCAGATGTCAAATGAGGAATCTTTTAC
pREPNTAP-zas1 rev	TTTTAGAGCTCGGTACCCGCGAAAATTAAGCAAAAAATACATAAAAAG
REPNTAP insertion seq fw	ACCCCAACTACTGCTTCTG
REPNTAP insertion seq rev	ACCCGTCTACGTTTCTAC
klf1 connect nmt NTAP to N' fw	CTTGATTATGGCGCGCCCCAT GGCAAGGGTATGACCAAGGCGAAAAAAAG
klf1 connect C' to Terminator rev	TCCATAGTTTGAAAGAAAAACCCTACTAAAGCTGTACTAATTTAGACAAAATGC
klf1 connect C' to terminator fw	GTCTAAATTAGTACAGCTTTAGTAGGGTTTTTCTTTCAAACTATGGAG
cnd1 connect nmt NTAP to N' fw	CTTGATTATGGCGCGCCCCATGGCAAGGGTATGTCGTTGGATCTTCTTTC
cnd1 connect C' to Terminator rev	TCCATAGTTTGAAAGAAAAACCCTATTATTCATGATATCCATCGTC
cnd1 connect C' to terminator fw	CGATGGATATCATGAATAATAGGGTTTTTCTTTCAAACTATGGAG
usp101 connect nmt NTAP to N' fw	CTTGATTATGGCGCGCCCCA TGGCAAGGGTATGGCTGAAAAATTACCG
usp101 connect C' to Terminator rev	TCCATAGTTTGAAAGAAAAACCCTA TCAATTGTAGCGACGACG
usp101 connect C' to terminator fw	CGTCGTCGCTACAATTGA TAGGGTTTTTCTTTCAAACTATGGAG
zas1 connect nmt NTAP to N' fw	CTTGATTATGGCGCGCCCCA TGGCAAGGGTATGTCAAATGAGGAATCTTTTACAG
zas1 connect C' to Terminator rev	TCCATAGTTTGAAAGAAAAACCCTA TTAATCATTTCCCTTGGATAATAATTG
zas1 connect C' to terminator fw	TATCCAAGGGAAATGATTAA TAGGGTTTTTCTTTCAAACTATGGAG
klf1 seq 1	AAGCCTTTATTTGCCCTCAC
klf1 seq 2	CTTCAATAAAAAACAATGCTAATAAGTC
klf1 seq 3	CTATACGCATCCAGATTTCAAG
klf1 seq 4	CGCCGATAGCTATGAAGC
klf1 seq 5	GTTTCTGCTTGGTTAGCTTC
1861 terminator connecting vector rev (for cDNA version)	CCGGGGATCCGTCGACATA CCGCATTACTAATAGAAAGGATTATTTCAC
usp101-PK tag fw 1	ATTTGGTCGTGGTCCTACTC GCTCCTCTCACTCTTCAGACTATGGAGGAAGAGATAGTTCCCCTAAGCGTCGTCGCTACAA T TCCGGTTCTGCTGCTAG
usp101-PK tag fw 2	TCCCGATTTCGTGGCGACTCTGGATTTCGTGGTGGCTATCGAGGAGGATTTCGAAAATCTT CTGGAGGAGGGTCAAG ATTTGGTCGTGGTCCTACTC
usp101-PK tag rev 1	TCGAAGAAAGAATGAGTAATCAAG AGTATACAAAAAATTATGTTTAGCGTTAACATTGAAGTGAGACTTTCTAACA GTTTAGCTTGCCTCGTCC
usp101-PK tag rev 2	AGCCAACTCATGGTACTTATTTAAATTTAGGCGTCTCCAATCTTCTATGCGCTTCTCCATT TTAACATGATAAC TCGAAGAAAGAATGAGTAATCAAG
usp101 tag seq	GATATGCATTTGTTGTGTTTG
Pcnd3 connect to hphMX fw	TCCAGTGTCGAAAACGAGCTCCCTACTACTGTGCACTCTACTAC
Pcnd3 connect to cnd1 rev	ATCCAACGACATATTCAATAACAATTATATTATGCCAATT
cnd1-connect to Pcnd3 fw	TTGTTATTGAATATGTCGTTGGATCTTCTTTC
cnd1-connect to Terminator rev	GTTTGAAAGAAAAACTTATTCATGATATCCATCGTC
Terminator connect to cnd1	GATATCATGAATAAGTTTTTCTTTCAAACTATGGAGC
Terminator connect to hphMX-rev	TATCATCGATGAATTCGAGCTGCATTACTAATAGAAAGGATTATTTC
TEF terminator seq	GCGTGATTTATATTTTTTTTCGCCTC

Acknowledgements

I here would like to firstly thank my supervisor Dr. Christian Häring for the research opportunity and allowing me to explore the topic independently. I also thank all the members of the Häring group- Christoph Schiklenk, Shveta Bisht, Maria Sol Bravo, Yuri Frosi, Fabian Merkel, Markus Hassler, Marc Kschonsak, Indra Alon Shaltiel, Lea Lecomte and Sumanjit Datta - for all the helpful discussions, advices and beautiful time. Special thank goes to Christoph Schiklenk for sharing his experiences and tips on fission yeast experiments. I also especially thank Shveta Bisht for all inspirations. I am very grateful for members in the Core Facility in EMBL who have made immense contributions to my project. I thank Diana Ordonez and Malte Paulsen in the Flow Cytometry Facility who have put great effort to facilitate me towards understanding my research subject. I thank Genomic Core Facility for their great service in DNA library preparation and sequencing. Especially, I thank Vladimir Benes. He is always keen for discussion and giving good advices to help me choose the suitable sequencing method. Bianka Baying in Gene Core also helped me a lot with patient explanations and discussions. I would like to sincerely thank Lin Gen for his tremendous effort in analyzing my experiment data and frequent discussions. I am so grateful for the S. pombe community, within which researchers from all over the world share their knowledge, resources and experiences without hesitate. In this context, I would like to specially thank Prof. Dr. Charles Hoffman (Boston College) who is always generous in helping scientists. He had kindly offered resource for my key experiment as gift and is always ready for answering my questions. I cannot express enough gratitude for all the help from Bähler lab (UCL) where all members are great sources of discussions as well as friendship. They have taught me how to perform SGA and provided great suggestions for further experiments. My time in EMBL was made enjoyable in large part due to many friends that I have met. I am honored to have friends as Giulia Paci, Jonas Hartman, Tiandi Yang and Yifan Yu who have offered me great support, memorable time and love. Last but not least, I give my sincere big thank to my family, my parents and Xiang, for all their love and encouragements. This work will not be possible without their great faithful support. Thank you.

Jin Wang

EMBL, Nov, 2018

References

Alberts B. et al., 2014. *Molecular Biology of The Cell*, sixth edition. Chapter 6, pp.299-368.

Anderson, D.E. et al., 2002. Condensin and cohesin display different arm conformations with characteristic hinge angles. *Journal of Cell Biology*, 156(3), pp.419–424.

Apolinario, E. et al., 1993. Cloning and manipulation of the Schizosaccharomyces pombe his7+ gene as a new selectable marker for molecular genetic studies. , 24(6), pp.491–495.

Aravind, L. et al., 2000. Lineage-specific loss and divergence of functionally linked genes in eukaryotes. *Proceedings of the National Academy of Sciences*, 97(21), pp.11319–11324.

Avery, L. & Wasserman, S., 2013. Ordering gene function: the interpretation of epistasis in regulatory hierarchies. , 18(9), pp.1199–1216.

Bähler, J., 2015. AnGeLi : A Tool for the Analysis of Gene Lists from Fission Yeast. , 6(November), pp.1–9.

Banecki, B. et al., 1996. Structure-function analysis of the zinc finger region of the DnaJ molecular chaperone. *Journal of Biological Chemistry*, 271(25), pp.14840–14848.

Bannister, A.J. & Kouzarides, T., 2011. Regulation of chromatin by histone modifications. *Cell Research*, 21(3), pp.381–395.

Baryshnikova, A. et al., 2010. *Synthetic genetic array (SGA) analysis in Saccharomyces cerevisiae and schizosaccharomyces pombe* 2nd ed., Elsevier Inc.

Basi, G., Schmid, E. & Maundrell, K., 1993. TATA box mutations in the Schizosaccharomyces pombe nmt1 promoter affect transcription efficiency but not the transcription start point or thiamine repressibility. *Gene*, 123(1), pp.131–136.

Braberg, H. et al., 2014. Quantitative analysis of triple-mutant genetic interactions. *Nature protocols*, 9(8), pp.1867–81.

Bresch, C., Müller, G. & Egel, R., 1968. Genes involved in meiosis and sporulation of a yeast. *MGG Molecular & General Genetics*, 102(4), pp.301–306.

Chang, C.-J., 2003. RNAi analysis reveals an unexpected role for topoisomerase II in chromosome arm congression to a metaphase plate. *Journal of Cell Science*, 116(23), pp.4715–4726.

Cheng, Z. et al., 2017. Overexpression of U1 snRNA induces decrease of U1 spliceosome function associated with Alzheimer's disease. *Journal of Neurogenetics*, 31(4), pp.337–343.

Christine. E. Brown, A.B.S., 1998. Poly(A) Tail Length Control in Saccharomyces cerevisiae Occurs by Message-Specific Deadenylation. *The Canadian Journal of Economics / Revue canadienne d'Economique*, 18(11), pp.6548–6559.

Collins, L.J. et al., 2009. The modern RNP world of eukaryotes. *Journal of Heredity*, 100(5), pp.597–604.

Cutter, A. & Hayes, J.J., 2016. A Brief Review of Nucleosome Structure. *FEBS Letters*, 589, pp.2914–2922.

Cuylen, S. et al., 2013. Short Article Entrapment of Chromosomes by Condensin Rings Prevents Their Breakage during Cytokinesis. *Developmental Cell*, 27(4), pp.469–78.

Cuylen, S., Metz, J. & Haering, C.H., 2011. Condensin structures chromosomal DNA through topological links. *Nature Structural &Amp; Molecular Biology*, 18, p.894.

Cyr, D.M., Langer, T. & Douglas, M.G., 1994. DnaJ-like proteins: molecular chaperones and specific regulators of Hsp70. *Trends in Biochemical Sciences*, 19(4), pp.176–181.

David Beach, 1982. Functionally homologous cell cycle control genes in budding and fission yeast. *Nature*, 300, pp.23–30.

Dixon, S.J. et al., 2008. Significant conservation of synthetic lethal genetic interaction networks between distantly related eukaryotes. *Proceedings of the National Academy of Sciences*, 105(43), pp.16653–16658.

Dixon, S.J. et al., 2009. Systematic mapping of genetic interaction networks. *Annu Rev Genet*, 43, pp.601–625.

Dovat, S. et al., 2002. A common mechanism for mitotic inactivation of C2H2 zinc finger DNA-binding domains. , pp.2985–2990.

Earnshaw, W.C. & Heck, M.M.S., 1985. Localization of topoisomerase II in mitotic chromosomes. *Journal of Cell Biology*, 100(5), pp.1716–1725.

Edens, L.J. et al., 2013. Nuclear size regulation: From single cells to development and disease. *Trends in Cell Biology*, 23(4), pp.151–159.

Egel, R., 1973. Commitment to meiosis in fission yeast. *MGG Molecular & General Genetics*, 121(3), pp.277–284.

Fantes, P.A., 1977. Control of cell size and cycle time in Schizosaharomyces pombe. *J. Cell. Sci.*, (24), pp.51–67.

Farlow, A. et al., 2015. The spontaneous mutation rate in the fission yeast Schizosaccharomyces pombe. *Genetics*, 201(2), pp.737–744.

Faustino, N.A., Cooper, T.A. & Andre, N., 2003. Pre-mRNA splicing and human disease. *Genes and Development*, 17(4), pp.419–437.

Forsburg, S.L., 1993. Comparison of Schizosaccharomyces pombe expression systems. , 21(12), pp.2955–2956.

Forsburg, S.L., 2001. The art and design of genetic screens: yeast. *Nature reviews. Genetics*, 2(9), pp.659–668.

Fudenberg, G. et al., 2017. Emerging Evidence of Chromosome Folding by Loop Extrusion. *Cold Spring Harbor Symposia on Quantitative Biology*, 82, pp.45–55.

Fudenberg, G. et al., 2016. Formation of Chromosomal Domains by Loop Extrusion. *Cell Reports*, 15(9), pp.2038–2049.

Gasser, S.M. et al., 1986. Metaphase chromosome structure. Involvement of topoisomerase II. *Journal of Molecular Biology*, 188(4), pp.613–629.

Giaever, G. et al., 2002. Functional profiling of the Saccharomyces cerevisiae genome. *Nature*, 418, p.387.

Gorbsky, G.J., 1994. Cell Cycle Progression and Chromosome Segregation in Mammalian Cells Cultured in the Presence of the Topoisomerase II Inhibitors ICRF-187. , 159(30), pp.3–9.

Gregan, J. et al., 2007. The Kinetochore Proteins Pcs1 and Mde4 and Heterochromatin Are Required to Prevent Merotelic Orientation. *Current Biology*, 17(14), pp.1190–1200.

Haber, J.E. et al., 2013. Systematic Triple-Mutant Analysis Uncovers Functional Connectivity between Pathways Involved in Chromosome Regulation. *Cell Reports*, 3(6), pp.2168–2178.

Hansen, J.C., 2002. Conformational Dynamics of the Chromatin Fiber in Solution: Determinants, Mechanisms, and Functions. *Annual Review of Biophysics and Biomolecular Structure*, 31(1), pp.361–392.

Hartman, J.L., Garvik, B. & Hartwell, L., 2001. Principles for the Buffering of Genetic Variation. *Science*, 291(5506), p.1001 LP-1004.

Heckman, D.S. et al., 2001. Molecular Evidence for the Early Colonization of Land by Fungi and Plants. *Science*, 293(5532), p.1129 LP-1133.

Hennessy, F. et al., 2005. Not all J domains are created equal- Implications for the specificity of Hsp40–Hsp70 interactions.pdf. , pp.1697–1709.

Hoffman, C.S., Wood, V. & Fantes, P.A., 2015. An ancient yeast for young geneticists: A primer on the Schizosaccharomyces pombe model system. *Genetics*, 201(2), pp.403–423.

Hofmann, J.C., Husedzinovic, A. & Gruss, O.J., 2010. The function of spliceosome components in open mitosis. *Nucleus*, 1(6), pp.447–459.

Hudson, D.F. et al., 2003. Condensin is required for nonhistone protein assembly and structural integrity of vertebrate mitotic chromosomes. *Developmental Cell*, 5(2), pp.323–336.

John C. Lucchesi, 1968. Synthetic lethality and semi-lethality among functionally related mutants of drosophila melanogaster. *Genetics*, 59(3), pp.37–44.

Kaida, D., 2016. The reciprocal regulation between splicing and 3′-end processing. *Wiley Interdisciplinary Reviews: RNA*, 7(4), pp.499–511.

Kaida, D. et al., 2010. U1 snRNP protects pre-mRNAs from premature cleavage and polyadenylation. *Nature*, 468(7324), pp.664–668.

Katherine C. Palozola, Greg Donahue, Hong Liu, Gregory R. Grant, Justin S. Becker, Allison Cote, Hongtao Yu, Arjun Raj, and K.S.Z., 2017. Mitotic Transcription and Waves of Gene Reactivation During Mitotic Exit. *Science*, 06(358), pp.119–122.

Kim, 2013. TopHat2 : accurate alignment of transcriptomes in the presence of insertions , deletions and gene fusions. *Genome Biology*, 14(4), pp.1–13.

Kim, D.-U. et al., 2010. Analysis of a genome-wide set of gene deletions in the fission yeast Schizosaccharomyces pombe. *Nature Biotechnology*, 28, p.617.

Kireeva, N. et al., 2004. Visualization of early chromosome condensation: A hierarchical folding, axial glue model of chromosome structure. *Journal of Cell Biology*, 166(6), pp.775–785.

Kirsten A. Hagstrom, 2002. C. elegans condensin promotes mitotic chromosome architecture, centromere organization, and sister chromatid segretation during mitosis and meiosis. *Genes & development*, 16(4), pp.729–742.

Kniola, B. et al., 2001. The Domain Structure of Centromeres Is Conserved from Fission Yeast to Humans. *Molecular Biology of the Cell*, 12(9), pp.2767–2775.

Kornblihtt, A.R. et al., 2013. Alternative splicing: A pivotal step between eukaryotic transcription and translation. *Nature Reviews Molecular Cell Biology*, 14(3), pp.153–165.

Kschonsak, M. et al., 2017. Structural Basis for a Safety-Belt Mechanism That Anchors Condensin to Chromosomes. *Cell*, 171(3), p.588–600.e24.

Kschonsak, M. & Haering, C.H., 2015. Shaping mitotic chromosomes: From classical concepts to molecular mechanisms. *BioEssays*, 37(7), pp.755–766.

Lammerding, J., 2011. Mechanics of the nucleus. *Comprehensive Physiology*, 1(2), pp.783–807.

Lee, M.G. & Nurse, P., 1987. Complementation used to clone a human homologue of the fission yeast cell cycle control gene cdc2. *Nature*, 327, p.31.

Linke, K. et al., 2003. The Roles of the Two Zinc Binding Sites in DnaJ. *Journal of Biological Chemistry*, 278(45), pp.44457–44466.

Lock, A. et al., 2018. PomBase 2018: user-driven reimplementation of the fission yeast database provides rapid and intuitive access to diverse, interconnected information. *Nucleic Acids Research*, (October 2017), pp.1–7.

Lorch, Y., LaPointe, J.W. & Kornberg, R.D., 1987. Nucleosomes inhibit the initiation of transcription but allow chain elongation with the displacement of histones. *Cell*, 49(2), pp.203–210.

Maeshima, K. & Eltsov, M., 2008. Packaging the genome: The structure of mitotic chromosomes. *Journal of Biochemistry*, 143(2), pp.145–153.

Maeshima, K. & Laemmli, U.K., 2003. A Two-step scaffolding model for mitotic chromosome assembly. *Developmental Cell*, 4(4), pp.467–480.

Martín-Castellanos, C. et al., 2005. A large-scale screen in S. pombe identifies seven novel genes required for critical meiotic events. *Current Biology*, 15(22), pp.2056–2062.

Matera, A.G. & Wang, Z., 2014. A day in the life of the spliceosome. *Nature Reviews Molecular Cell Biology*, 15(2), pp.108–121.

Matsuo, Y. et al., 2006. A Rapid Method for Protein Extraction from Fission Yeast. *Bioscience, Biotechnology, and Biochemistry*, 70(8), pp.1992–1994.

Matthieu Piel, 2009. Cell shape and cell division in fission yeast minireview. , 15(19(17)), pp.823–827.

Maundrell, K., 1990. nmtl of Fission Yeast. *Journal of Biological Chemistry*, 265(19), pp.10857–10864.

McKie, A.B., 2001. Mutations in the pre-mRNA splicing factor gene PRPC8 in autosomal dominant retinitis pigmentosa (RP13). *Human Molecular Genetics*, 10(15), pp.1555–1562.

Mroczek, S. & Dziembowski, A., 2013. U6 RNA biogenesis and disease association. *Wiley Interdisciplinary Reviews: RNA*, 4(5), pp.581–592.

Neuwald, A.F. & Hirano, T., 2000. HEAT repeats associated with condensins, cohesins, and other complexes involved in chromosome-related functions. *Genome Research*, 10(10), pp.1445–1452.

Newo, A.N.S. et al., 2007. Proteomic analysis of the U1 snRNP of Schizosaccharomyces pombe reveals three essential organism-specific proteins. *Nucleic Acids Research*, 35(5), pp.1391–1401.

Noguchi, E. & Forsburg, S.L., 2009. Measuring DNA content by Flow Cytometry in Fission Yeast. *Methods in molecular biology (Clifton, N.J.)*, 521, pp.493–507.

Nurse, P., 2000. A long twentieth century of the cell cycle and beyond. *Cell*, 100(1), pp.71–78.

Nurse, P. & Bissett, Y., 1981. Gene required in G1 for commitment to cell cycle and in G2 for control of mitosis in fission yeast. *Nature*, 292, p.558.

Ohtani, M., 2017. Transcriptional regulation of snRNAs and its significance for plant development. *Journal of Plant Research*, 130(1), pp.57–66.

Ohtsuka, K. & Hata, M., 2000. Molecular chaperone function of mammalian Hsp70 and Hsp40 - A review. *International Journal of Hyperthermia*, 16(3), pp.231–245.

Okazaki, K. & Niwa, O., 2000a. mRNA Encoding Zinc Finger Protein Isoforms are Expressed by Alternative Splicing of an In-frame Intron in Fission Yeast. , 7, pp.27–30.

Okazaki, K. & Niwa, O., 2000b. mRNAs encoding zinc finger protein isoforms are expressed by alternative splicing of an in-frame intron in fission yeast. *DNA Res.*, 30, pp.27–30.

Onn, I. et al., 2007. Reconstitution and subunit geometry of human condensin complexes. *The EMBO journal*, 26(4), pp.1024–34.

Ou, H.D. et al., 2017. ChromEMT: Visualizing 3D chromatin structure and compaction in interphase and mitotic cells. *Science*, 357(6349).

Patel, S.B. & Bellini, M., 2008. The assembly of a spliceosomal small nuclear ribonucleoprotein particle. *Nucleic Acids Research*, 36(20), pp.6482–6493.

Paul Nurse, 1975. Genetic control of cel size at cell division in yeast. *Nature*, 256, pp.547–551.

Petrova, B. et al., 2013. Quantitative analysis of chromosome condensation in fission yeast. *Molecular and cellular biology*, 33(5), pp.984–98.

Převorovský, M. et al., 2015. Fission yeast CSL transcription factors: Mapping their target genes and biological roles. *PLoS ONE*, 10(9), pp.1–23.

Rabitsch, K.P. et al., 2003. Kinetochore recruitment of two nucleolar proteins is required for homolog segregation in meiosis I. *Developmental Cell*, 4(4), pp.535–548.

Rallis, C., Townsend, S. & Bähler, J., 2017. Genetic interactions and functional analyses of the fission yeast gsk3 and amk2 single and double mutants defective in TORC1-dependent processes. *Scientific Reports*, 7(March), pp.1–11.

Rea, S. et al., 2000. Regulation of chromatin structure by site-specific histone H3 methyltransferases. *Nature*, 406, p.593.

Richmond, T.J., 1984. Structure of the nucleosome core particle at 7 A resolution. *Nature*, 311, pp.532–537.

Rodriguez, F. et al., 2008. Molecular Basis for Regulation of the Heat Shock Transcription Factor σ32by the DnaK and DnaJ Chaperones. *Molecular Cell*, 32(3), pp.347–358.

Roguev, A. et al., 2007. High-throughput genetic interaction mapping in the fission yeast Schizosaccharomyces pombe. *Nature Methods*, 4(10), pp.861–866.

Roguev, A. et al., 2003. High conservation of the Set1/Rad6 axis of histone 3 lysine 4 methylation in budding and fission yeasts. *Journal of Biological Chemistry*, 278(10), pp.8487–8493.

Ryan, C.J. et al., 2012. Hierarchical Modularity and the Evolution of Genetic Interactomes across Species. , pp.691–704.

Sami Hocine, Robert H. Singer, D.G., 2010. RNA Processing and Export. *Water Resources*, 2, p.a000752.

Sanchez, R. & Zhou, M.M., 2011. The PHD finger: A versatile epigenome reader. *Trends in Biochemical Sciences*, 36(7), pp.364–372.

Schiklenk, C. et al., 2018. Control of mitotic chromosome condensation by the fission yeast transcription factor Zas1. *The Journal of Cell Biology*, 217(7), pp.2383–2401.

Shimanuki, M. et al., 2013. Klf1, a C2H2 Zinc Finger-Transcription Factor, Is Required for Cell Wall Maintenance during Long-Term Quiescence in Differentiated G0 Phase. *PLoS ONE*, 8(10), pp.1–14.

Sipiczki, M., 2000. Where does fission yeast sit on the tree of life ? Mycota. *Genome Biology*, 1(2), pp.1–4.

Soni, S. et al., 2014. Transcription factor EKLF (KLF1) recruitment of the histone chaperone HIRA is essential for β-globin gene expression. *Proceedings of the National Academy of Sciences*, 111(37), pp.13337–13342.

Strzyz, P., 2018. Chromosome biology: A stairway to mitotic chromosome assembly. *Nature Reviews Molecular Cell Biology*, 19(3), pp.139–139.

Styrkfirsdttir, U., Egel, R. & Nielsen, O., 1993. The smt-0 mutation which abolishes mating-type switching in fission yeast is a deletion. *Current Genetics*, 23, pp.184–186.

Suzuki, H. et al., 2012. Synergistic binding of DnaJ and DnaK chaperones to heat shock transcription factor σ^{32} ensures its characteristic high metabolic instability: Implications for heat shock protein 70 (Hsp70)-Hsp40 mode of function. *Journal of Biological Chemistry*, 287(23), pp.19275–19283.

Szabo, A. et al., 1996. A zinc finger-like domain of the molecular chaperone DnaJ is involved in binding to denatured protein substrates. *The EMBO Journal*, 15(2), pp.408–417.

Tada, K. et al., 2011. Condensin association with histone H2A shapes mitotic chromosomes. *Nature*, 474(7352), pp.477–485.

Takahashi, H. et al., 2015. MED26 regulates the transcription of snRNA genes through the recruitment of little elongation complex. *Nature Communications*, 6, pp.1–15.

Tasto, J.J. et al., 2001. Vectors and gene targeting modules for tandem affinity purification in Schizosaccharomyces pombe. *Yeast*, 18(7), pp.657–662.

Tong, A.H.Y. et al., 2001. Systematic Genetic Analysis with Ordered Arrays of Yeast Deletion Mutants. *Science*, 294(5550), p.2364 LP-2368.

Vagnarelli, P. et al., 2006. Condensin and Repo-Man–PP1 co-operate in the regulation of chromosome architecture during mitosis. *Nature Cell Biology*, 8, p.1133.

Valerie Wood, 2016. How to get the most from fission yeast genome data: a report from the 2006 European Fission Yeast Meeting Computing Workshop. *Yeast*, 23, pp.905–912.

Vazquez-Arango, P. & O'Reilly, D., 2018. Variant snRNPs: New players within the spliceosome system. *RNA Biology*, 15(1), pp.17–25.

Vignali, M. et al., 2000. MINIREVIEW ATP-Dependent Chromatin-Remodeling Complexes. , 20(6), p.1899.

Wagih, O. et al., 2013. SGAtools: One-stop analysis and visualization of array-based genetic interaction screens. *Nucleic acids research*, 41(Web Server issue), pp.591–596.

Wahl, M.C., Will, C.L. & Lührmann, R., 2009. The Spliceosome: Design Principles of a Dynamic RNP Machine. *Cell*, 136(4), pp.701–718.

Walsh, P. et al., 2004. The J-protein family: Modulating protein assembly, disassembly and translocation. *EMBO Reports*, 5(6), pp.567–571.

Wang, L. et al., 2005. Schizosaccharomyces pombe adenylate cyclase suppressor mutations suggest a role for cAMP phosphodiesterase regulation in feedback control of glucose/cAMP signaling. *Genetics*, 171(4), pp.1523–1533.

Wood, V. et al., 2002. The genome sequence of Schizosaccharomyces pombe. *Nature*, 415, p.871.

Wood, V. & Nurse, P., 2002. The genome sequence of Schizosaccharomyces pombe. *Nature*, 415(February), pp.871–880.

Yamazaki, T. et al., 2012. FUS-SMN Protein Interactions Link the Motor Neuron Diseases ALS and SMA. *Cell Reports*, 2(4), pp.799–806.

Yu, Y. et al., 2015. U1 snRNP is mislocalized in ALS patient fibroblasts bearing NLS mutations in FUS and is required for motor neuron outgrowth in zebrafish. *Nucleic Acids Research*, 43(6), pp.3208–3218.